RM L55E20

RESEARCH MEMORANDUM

A THEORETICAL INVESTIGATION OF A COMPENSATING NETWORK WITH APPLICATION TO ROLL CONTROL SYSTEMS FOR AUTOMATIC INTERCEPTORS

By Windsor L. Sherman

Langley Aeronautical Laboratory
Langley Field, Va.

NATIONAL ADVISORY COMMITTEE
FOR AERONAUTICS

WASHINGTON

July 21, 1955
Declassified May 16, 1958

NATIONAL ADVISORY COMMITTEE FOR AERONAUTICS

RESEARCH MEMORANDUM

A THEORETICAL INVESTIGATION OF A COMPENSATING NETWORK WITH APPLICATION TO ROLL CONTROL SYSTEMS FOR AUTOMATIC INTERCEPTORS

By Windsor L. Sherman

SUMMARY

A theoretical analysis of an airplane automatic control system incorporating a compensating network is presented. The compensating network is a computing network that has characteristics that are the inverse of the airframe; consequently, airplane dynamics are eliminated from the system response. The transfer function of this type of control is developed, and the result is applied to the analysis of roll control systems. The basic roll control system is a displacement or bank-angle control system. This basic system was modified by feeding back rolling velocity and acceleration to the input of the compensating network to obtain velocity and acceleration control systems. In addition to the linear analysis, an analog-computer study was made to determine the effects of limiting the control-surface rate and displacement and of incomplete compensation on the command response of the roll control systems.

The results are presented in the form of time histories of the lateral airplane variables and control-surface motions.

For the forward-loop compensating network, the effects produced by limiting and incomplete compensation on the response characteristics of the system indicate that the system cannot at present be considered as a satisfactory automatic control system for interceptor airplanes.

INTRODUCTION

The manned all-weather interceptor has assumed an important role as an air defense weapon. Since it is anticipated that the interceptor may be automatically controlled in the attack phase of the intercept mission, an effective automatic control system is a necessary component

of the automatic interceptor system. The interceptor airframe, as presently conceived, is a monowing design that rolls to turn toward the interception point. Therefore, an automatic roll control system is a necessary part of the guidance system for these interceptors. As part of a general investigation of the attack phase of the automatic interceptor, a roll control system incorporating a compensating network has been studied.

Reference 1 proposes the use of a compensating network, as part of an automatic pilot, to compensate all or part of the lateral and longitudinal modes of the airframe. Compensating networks that wholly or partially cancel the longitudinal modes of the airframe, when controlled by a human pilot, have been discussed in references 2 and 3.

The compensating network, as used in the roll control system of the present investigation, is a control-deflection computer designed to eliminate the lateral modes of motion from the response of the system to a command input. If the roll control system operates in a linear manner and if the compensating network is correctly designed, cancellation of the airframe dynamics is always obtained. However, in this investigation physical limits were imposed on control-surface rate and displacement; thus the system became nonlinear. Also, small inaccuracies in the mass and aerodynamic data required to design the compensating network and changes in the airplane flight condition were used to introduce incomplete compensation into the system operation. The effect of these nonlinearities and inaccuracies on the behavior of the system in response to command inputs for a forward-loop compensating network is discussed in this paper.

The results are presented as time histories of the lateral motions of the interceptor and control-surface motions, which were obtained on the Reeves Electronic Analog Computer (REAC) at Project Cyclone and at the Langley Aeronautical Laboratory. Some of these results have been previously summarized in reference 4.

SYMBOLS

t	time, sec
D	differential operator, $\frac{d}{dt}$
a	arbitrary constant in exponential input $\phi_c(1 - e^{-at})$
$F(D)$	compensating-network transfer function, forward loop

$F_1(D)$	compensating-network transfer function, feedback loop
$S(D)$	first-order-servo transfer function
$S_1(D)$	integrating-servo transfer function, $S_1(D) = \frac{1}{D} S(D)$
$G(D)$	primary airplane transfer function
$N(D)$	numerator of $G(D)$
$\delta(D)$	denominator of $G(D)$
$G_1(D)$	secondary airplane transfer function
n	exponent of integrator in compensating network
$\eta(D)$, $X(D)$	degrees of freedom of airplane
M	externally applied disturbance function
$O(D)$	output of feedback-loop compensating network
τ	servo time constant, sec
K	compensating-network gain constant
$R(D)$	arbitrary polynomial defining airplane response, used in feedback-loop compensating network
K_1	velocity-command gain constant, sec^{-1}
K_2	acceleration-command gain constant, sec^{-1}
b	wing span, ft
S	wing area, sq ft
μ	relative density factor, $\frac{m}{\rho S b}$
m	mass of airplane, W/g, slugs
W	weight, lb
g	acceleration due to gravity, ft/sec^2
K_X	nondimensional radius of gyration in roll about longitudinal stability axis, $\sqrt{K{X_o}^2 \cos^2\eta + K{Z_o}^2 \sin^2\eta}$

K_Z nondimensional radius of gyration in yaw about vertical stability axis, $\sqrt{K_{Z_o}^2\cos^2\eta + K_{X_o}^2\sin^2\eta}$

K_{XZ} nondimensional product of inertia, $\left(K_{X_o}^2 - K_{Z_o}^2\right)\sin\eta\cos\eta$

K_{X_o} nondimensional radius of gyration about principal X body axis of airplane

K_{Z_o} nondimensional radius of gyration about principal Z body axis of airplane

ϕ roll angle of airplane

β sideslip angle of airplane

ψ yaw angle of airplane

α angle of attack

η inclination of principal longitudinal axis with respect to flight path

γ flight-path inclination from horizontal, $\theta - \alpha$

δ_a aileron deflection angle

p rolling angular velocity, radians/sec

r yawing angular velocity, radians/sec

H altitude, ft

ρ mass density of air, slugs/cu ft

V true airspeed, ft/sec

M Mach number

C_l rolling-moment coefficient, $\frac{\text{Rolling moment}}{qSb}$

C_n yawing-moment coefficient, $\frac{\text{Yawing moment}}{qSb}$

C_Y lateral-force coefficient, $\frac{\text{Lateral force}}{qS}$

C_L trim lift coefficient

$$C_{l_p} = \frac{\partial C_l}{\partial\left(\frac{pb}{2V}\right)}$$

$$C_{n_p} = \frac{\partial C_n}{\partial\left(\frac{pb}{2V}\right)}$$

$$C_{Y_p} = \frac{\partial C_Y}{\partial\left(\frac{pb}{2V}\right)}$$

$$C_{l_r} = \frac{\partial C_l}{\partial\left(\frac{rb}{2V}\right)}$$

$$C_{n_r} = \frac{\partial C_n}{\partial\left(\frac{rb}{2V}\right)}$$

$$C_{Y_r} = \frac{\partial C_Y}{\partial\left(\frac{rb}{2V}\right)}$$

$$C_{l_\beta} = \frac{\partial C_l}{\partial \beta}$$

$$C_{n_\beta} = \frac{\partial C_n}{\partial \beta}$$

$$C_{Y_\beta} = \frac{\partial C_Y}{\partial \beta}$$

Subscripts:

i	input
o	output
l	limiting value of a variable

A dot over a symbol indicates differentiation with respect to time; for example, $\dot{\phi} = \frac{d\phi}{dt}$.

All angles are measured in radians unless otherwise noted.

BASIC CONSIDERATIONS

The automatic control system studied in this investigation incorporates a compensating network, a device that eliminates airplane dynamics from the system response. The compensating network is essentially a computer that solves a set of equations that are the inverse of the equations of motion of the airplane. The input to the network is either an angular displacement, velocity, or acceleration and the output is the control-surface deflection required to give the input value of the variable.

Figure 1 presents the block diagram of an automatic control system incorporating a forward-loop compensating network. The dynamic response of this system is studied by a linear analysis and by simulation on an analog computer where nonlinearities and imperfect compensation were introduced into the problem. Inasmuch as the regulatory response characteristics, the return of the airplane to a specified steady-state condition when disturbed from that condition by an externally applied moment, may be of some interest, this type of control-system operation was studied in addition to the command-response dynamics. Appendix A presents the theoretical analysis of the forward-loop compensating-network type of control system and the transfer function is developed. In addition, the feedback-loop compensating network is subjected to a brief analytical study in appendix A. This type of compensating-network control system appears to eliminate some of the disadvantages of the forward-loop compensating network but mechanization difficulties may bar it as a practical system.

Application of the Compensating Network to Roll Control Systems

In order to evaluate a specific application of the compensating network for the automatic control of airplanes, the principles set forth in appendix A were applied to three automatic roll control systems. These roll control systems differ in the number and types of feedback used and in this report the roll control systems are identified by the highest order feedback used. Thus the basic control system (fig. 2(a)) is a displacement control or bank-angle-feedback system. The second system (fig. 2(b)), herein called the velocity control system, is derived from the first by the addition of a rolling-velocity feedback and a gain K_1. The third system (fig. 2(c)), called the acceleration control system, was obtained by adding a rolling-acceleration feedback and a gain K_2 to the velocity control system.

In a compensating network control-system feedbacks are not required, as in other types of control systems, to add damping and thereby improve the system response, since the cancellation of the airplane dynamics

eliminates the problems of poor airplane stability and damping. Thus, feedbacks are always made to the input side of the compensating network, since feedbacks to the servo for additional damping are unnecessary and if made would destroy the cancellation of the airplane dynamics. The feedbacks shown in figure 2 are used to determine the airplane variable - bank angle, rolling velocity, or rolling acceleration - that is used in the compensating network to compute the desired control-surface deflection. This value of δ is determined so that airplane dynamics are eliminated from the system response as the airplane assumes the value of the variable that is fed to the compensating network.

Since these roll control systems are considered as a part of a complete interceptor system, it is desirable to correlate the simulation used for the roll control systems with the automatic interceptor system. In an actual interceptor system the outputs of the airborne radar and director computer determine an azimuth error and an elevation error. These errors are used in the command computer to define a roll command and a normal-acceleration command. The roll command depends upon the particular type of guidance system used and may be either a desired bank angle in space coordinates or a bank-angle error in interceptor coordinates. If an interceptor system is designed to command a bank angle in space coordinates, the bank-angle feedback is a necessary part of the roll control system. Therefore, in order to simulate this system, the radar and computers need only be replaced by a bank-angle input to obtain a simple analog of the more complex system. However, if the radar-computer system operates in interceptor coordinates, the system is closed by a feedback loop through the radar. In this case the basic command to the roll control system is a rolling-velocity command that is proportional to the azimuth and elevation errors. Therefore, replacing the radar and computer by a bank-angle input, a bank-angle feedback, and a gain to convert the bank-angle error to a rolling-velocity command constitutes the first approximation to the analog of the more complex system. Thus, the roll control systems shown in figure 2 are applicable to either one of the two guidance systems mentioned above.

Simulator Setup

Airplane equations of motion.- All airplane transfer functions, and consequently the transfer function of the compensating network, used in this investigation were derived from the linear equations of lateral motion with $\gamma = 0$, which are as follows:

$$\left.\begin{aligned}
&\left[2\mu K_Z{}^2\left(\frac{b}{V}\right)^2 D^2 - \frac{b}{2V} C_{n_r} D\right]\psi - \left[2\mu K_{XZ}\left(\frac{b}{V}\right)^2 D^2 + \frac{b}{2V} C_{n_p} D\right]\phi - C_{n_\beta}\beta = 0 \\
&-\left[2\mu K_{XZ}\left(\frac{b}{V}\right)^2 D^2 + \frac{b}{2V} C_{l_r} D\right]\psi + \left[2\mu K_X{}^2\left(\frac{b}{V}\right)^2 D^2 - \frac{b}{2V} C_{l_p} D\right]\phi - C_{l_\beta}\beta = C_{l_{\delta_a}}\delta_a \\
&\left(2\mu \frac{b}{V} D - \frac{b}{2V} C_{Y_r} D\right)\psi - \left(\frac{b}{2V} C_{Y_p} D + C_L\right)\phi + \left(2\mu \frac{b}{V} D - C_{Y_\beta}\right)\beta = 0
\end{aligned}\right\} \quad (1)$$

The general form of the airplane transfer function $G(D)$ is

$$G(D) = \frac{\phi(D)}{\delta_a(D)} = \frac{a_1 D^2 + a_2 D + a_3}{b_1 D^4 + b_2 D^3 + b_3 D^2 + b_4 D + b_5} \quad (2)$$

In equation (2) the coefficients a_1 to a_3 and b_1 to b_5 are functions of the mass and aerodynamic characteristics of the airplane and can be obtained by expanding the determinant of the airplane equations of motion, which is obtained from equations (1).

Flight condition A, presented in table I, is the standard flight condition used in both the airframe and compensating-network equations when perfect compensation was desired. Incomplete compensation was introduced, aerodynamically, by substituting the singular or group variations (flight condition A-1 or A-2) into the airplane equations. When it was desired to use two flight conditions in the problem, flight condition A remained in the compensating network and flight condition B of table I was used in the airplane equations of motion.

Compensating network.- The generalized transfer function of the compensating network is

$$F(D) = \frac{K}{D^n G(D)} \quad (3)$$

where $G(D)$ is the transfer function ϕ/δ_a of the airplane (eq. (2)), K is the gain or amplification through the network, $1/D$ is an integrator, and the exponent n prescribes the order of integration. In general, the maximum value of n that can be used is one greater than the highest order of the derivative of the bank angle that is fed back to form the input to the compensating network (see fig. 2).

The servo.- The servo used through the investigation is a first-order time-lag servo, defined by equation (A1). The servo time constant τ is one of the variables of the investigation.

Limiting was applied to the servo to simulate control-surface rate and displacement restrictions of a physical system. Two types of limiters were used, the winding and nonwinding types of limiters. When δ, the control-surface angular displacement, does not reach its limit, both types of limiters operate in an identical manner, even though $\dot{\delta}$, the control-surface angular rate, is limited. However, when δ reaches its limit, important differences occur in the operation of these limiters. In the winding-type limiter, when $\delta \geqq \delta_l$ the following condition

$$\int_0^t \dot{\delta}\, d\tau < \delta_l \tag{4}$$

must be satisfied before δ can move off the stop. In the nonwinding type of limiter for $\delta \geqq \delta_l$

$$\left.\begin{aligned} &\int_0^t \dot{\delta}\, d\tau = \delta_l \\ &\dot{\delta} = 0 \end{aligned}\right\} \tag{5}$$

which implies that for $\dot{\delta} < 0$, δ moves off the stop immediately. It should be noted that the above discussion applies to positive limits. An equivalent representation can be written for the negative limits. These two types of limiters were included in the study because it was felt that winding limiters more closely approximate the operating characteristics of the proportional servo and its stroking motor when they are operating in a saturated condition, whereas the nonwinding limiter represents a perfect proportional servo and stroking motor.

The nonwinding-type limiter as used in this problem was set up so that $\dot{\delta}$ goes to zero when δ is limited. This return to zero by $\dot{\delta}$ was not carried through to the recorders; consequently, $\dot{\delta}$ always shows a value on the record whether or not δ is limited. Therefore, in order to determine when $\dot{\delta}$ is limited from these records for the nonwinding limiter, the behavior of δ must be taken into account as well as the behavior of $\dot{\delta}$.

SCOPE

The investigation included both a linear analysis and a REAC study of the three types of roll control systems. The main purpose of the linear analysis is to show the effect of the system gains and servo time constant on the roll response of the airplane to a command input. The REAC study was conducted to investigate the effect of incomplete compensation and nonlinearities.

Incomplete compensation results when the transfer function of the compensating network is not the exact inverse of the airplane transfer function. In the REAC simulation, incomplete compensation was introduced by changing the airplane flight condition from the flight condition for which the compensating network was designed and also by varying the stability derivatives singly and in combination in the airplane transfer function as shown in flight conditions A-1 and A-2 of table I. The latter simulates the problem which may arise in practice, where the compensating-network design is based on estimated stability derivatives, and the resulting network transfer function is not the exact inverse of the actual airplane transfer function. The nonlinearities incorporated in the system are limits imposed on the maximum values of control-surface rate and displacement.

RESULTS AND DISCUSSION

General

The transfer functions used in the linear analysis of these control systems were derived as outlined in appendix A, assuming perfect compensation and linear operating conditions. The transfer function for each of these systems is as follows:

For the displacement control system

$$\frac{\phi_o}{\phi_i} = \frac{K}{D^n(1 + \tau D) + K} \tag{6}$$

For the velocity control system

$$\frac{\phi_o}{\phi_i} = \frac{KK_1}{D^n(1 + \tau D) + KD + KK_1} \tag{7}$$

For the acceleration control system

$$\frac{\phi_o}{\phi_i} = \frac{KK_1K_2}{D^n(1 + \tau D) + KD^2 + KK_2D + K_1K_2K} \tag{8}$$

Routh's discriminant was applied to the characteristic equation of each of these systems. Unstable conditions were indicated as follows:

For the displacement control system

$$n > 1 \tag{9}$$

For the velocity control system

$$\left.\begin{aligned} &n > 2 \\ &K_1 < \frac{1}{2} \qquad (n = 2) \end{aligned}\right\} \tag{10}$$

For the acceleration control system

$$\left.\begin{aligned} &n > 3 \\ &K < K_1\tau - 1 \qquad (n = 2) \\ &K < \frac{K_1}{1 - \tau K_2} \qquad (n = 3) \end{aligned}\right\} \tag{11}$$

In addition, system stability requires that all gains be positive.

The rise time (the time required to reach 90 percent of the steady-state value) and the response time (the time required for the motions to reach and remain within 5 percent of the steady-state value) were used to analyze system responses and to make comparisons of different operating conditions. The linear analysis was used to determine the effects of varying the gains and servo time constant on the command response of the system. The variations were checked on the REAC and it was found that, when no limiting was present, there was good agreement between the linear and REAC results. However, when n, the exponent of the compensating network, is equal to 1 and a step input is used, initial conditions arise in the problem that destroy compensation. This situation, with REAC records, is discussed in the section on the displacement control system, and an analysis of this condition for the same control system is presented in appendix B. When limiting of the control-surface rate and displacement was added, the problem became nonlinear. The REAC was used to investigate this phase of the problem. Therefore, only REAC records showing the

effect of varying the limits on the control-surface rate and displacement are presented in this report.

Equation (A6) partially predicts the limiting condition introduced by increasing the gains because it shows that the forward-loop gain appears as a multiplicative factor in the amplitudes of δ and $\dot{\delta}$.

In general, the comments relative to the gains apply in the same way when τ, the servo time constant, is varied. However, REAC results indicate that the value of τ that is optimum in the linear analysis may not be the best when the control-surface rate and displacement are limited. For the displacement control system, where limiting is present, the oscillations introduced by τ combine with the oscillations caused by the rate limiting to produce a system response that approaches the linear result. This effect is shown in figure 3.

When the roll response of the airplane is compensated, the β and $\dot{\psi}$ motions are uncompensated. This occurs, as indicated by equation (A6), because airplane characteristics appear as a factor of the characteristic equation of the β and $\dot{\psi}$ transfer functions.

Incomplete compensation was introduced by changing the stability derivatives individually or in groups or by changing the flight condition as indicated in table I. The resulting system response was in general unsatisfactory. However, in the case of the $n = 3$ acceleration control system, a satisfactory system response was obtained for the mixed-flight-condition type of incomplete compensation. More detailed results of this study are presented in the sections on the displacement and acceleration control systems. The regulatory response for the basic control system and the two variations studied were uncompensated, as indicated by equation (A8). Although the response was uncompensated, it showed stable characteristics. For the magnitude of the disturbances considered ($C_l = C_n = 0.1$) limiting of the control-surface rate and displacement was troublesome only at high values of the forward-loop gain or servo time constant, or both. Since the regulatory response was uncompensated, this mode of control-system operation was not extensively investigated and no results are presented.

The linear analysis and the REAC investigation of the effects of limiting are presented in the following sections for each of the control-system variations considered. When applicable, results on incomplete compensation are also presented.

The Displacement Control System

Linear analysis.- Equation (6) subject to condition (9) was used to determine the effect of varying K and τ on the response of the linear system. A step function, $\phi_i = 60^\circ$, was used as the command input.

Figure 4 shows that, as K is increased from 5 to 12, both the rise time and the response decrease. As τ is increased from 0.01 to 0.3 second (fig. 5), an oscillatory mode is introduced into the system response. An examination of the characteristic equation of the system indicates that these oscillations occur for $\tau > \frac{1}{4K}$ and that the frequency of the oscillations is proportional to $\frac{1}{2\tau}\sqrt{1 - 4K\tau}$.

REAC study.- In order to evaluate the effects of limiting and incomplete compensation, the control system was set up on an REAC type of analog computer. To check the REAC setup, a run was made under linear conditions. A step input of $\phi_i = 60^\circ$ was applied to the system and, inasmuch as no limiting occurs, the ϕ motion shown in figure 6(a) should be directly comparable with the linear curve in figure 6(b). A comparison of these two curves shows that the frequencies and rise times of the two motions are radically different. An examination of the equations of motion of this control system indicated that initial conditions arising in the compensating network from the use of the step input were causing incomplete compensation. The analysis presented in appendix B shows that, in order for complete compensation to take place, $\phi_i(0) \equiv 0$. The command-input network was changed so $\phi_i(t) = \phi_c(1 - e^{-at})$ and ϕ_c was set equal to 60°. Figure 7 shows the time histories of the recorded variables for the exponential input. A comparison of the ϕ motion with that shown in figure 6(b) shows that the linear and REAC results are now in approximate agreement.

As indicated by equation (A6), the motions $\dot{\psi}$, β, δ, and $\dot{\delta}$ due to ϕ_i, shown in figure 7, will be uncompensated and contain the oscillatory characteristics determined from $(\tau D^2 + D + K)(a_1 D^2 + a_2 D + a_3)$ which is the characteristic equation of the system. Thus, in addition to oscillatory modes that come from the control system, oscillatory characteristics determined by $a_1 D^2 + a_2 D + a_3$, the numerator of $G(D)$, will also be present in the $\dot{\psi}$ and β motions. In terms of the mass and aerodynamic characteristics of the airplane, the coefficients a_1, a_2, and a_3 are

$$a_1 = 4\mu^2 K_Z^2 \left(\frac{b}{V}\right)^2 C_{l_{\delta_a}}$$

$$a_2 = -\frac{b}{V}\mu\left(2K_Z^2 C_{Y_\beta} + C_{n_r}\right)C_{l_{\delta_a}}$$

$$a_3 = \left(2\mu C_{n_\beta} - \frac{1}{2}C_{Y_r}C_{n_\beta} + \frac{1}{2}C_{n_r}C_{Y_\beta}\right)C_{l_{\delta_a}}$$

For the airplane and control system studied herein, the airplane induced oscillations are predominant. The period of the airplane oscillation, for the flight condition considered, is 1.65 seconds, which is very close to the period of the Dutch roll oscillation.

The effect of limiting δ and $\dot{\delta}$: The effect of limiting $\dot{\delta}$ and δ was studied by using the nonwinding type of limiter. Comparing figure 7 where $\dot{\delta}$ is unlimited with figures 8(a) and 8(b) where $\dot{\delta}_l$ is set at 100 deg/sec and 50 deg/sec, respectively, shows that the effect of limiting $\dot{\delta}$ is to introduce a low initial peak and an oscillation in the ϕ motion. Further reductions in $\dot{\delta}_l$ cause more limiting to occur, which in turn causes the severity of the limiting-induced oscillation to increase.

When δ is limited and $\dot{\delta}_l$ held constant, the effects are the same as noted for limiting of $\dot{\delta}$. As δ_l is reduced from 20° to 10° (figs. 9(a) and 9(b)), the amplitude of the oscillations increases. Setting δ_l equal to 5° (see fig. 9(c)) causes the entire pattern of the oscillations to change. The δ motion now approximates a square wave. The high-frequency oscillation in the ϕ and $\dot{\phi}$ responses is the third harmonic of the basic frequency of the δ square wave, the second term of the Fourier series for a square wave, and disappears as soon as the δ square wave decays. A reduction in $\dot{\delta}_l$ to 40 deg/sec (fig. 9(d)) produced no major change in the motion observed in figure 9(c), where $\delta_l = 5°$ and $\dot{\delta}_l = 100$ deg/sec. Thus, it appears that, for small values of δ_l, the effect of reducing $\dot{\delta}_l$ is not critical.

Incomplete compensation: The aerodynamic stability derivatives of the airplane were varied singly and as a group as shown in table I. Only two of the derivatives, C_{n_β} and C_{l_β}, produced a noticeable effect on the system response, the effect of C_{n_β} being more pronounced than the effect of C_{l_β}. When C_{n_β} was increased to 0.32 (fig. 10(a)), a very lightly damped hunting oscillation was introduced in the ϕ and $\dot{\phi}$ responses. The characteristics of this oscillation and its effect on the response time are such that the system response is considered unsatisfactory.

Decreasing C_{n_β} to 0.25 or increasing C_{l_β} to -0.08 had the same effect on the system response. Figure 10(b) shows an example of this effect on the system response for $C_{l_\beta} = -0.08$. This oscillation is less persistent than the one introduced by increasing C_{n_β} (fig. 10(a)). However, comparing the system responses for $C_{l_\beta} = -0.08$ with a similar case for $C_{l_\beta} = -0.106$ (fig. 9(a)) shows that the oscillations in the ϕ and $\dot{\phi}$ motions are more lightly damped for the incomplete-compensation

case (fig. 10(b)). Decreasing C_{l_β} to -0.13 produces a negligible effect on the system response.

When the flight condition of the airplane was changed from flight condition A to flight condition B (table I), the oscillation shown in figure 10(c) occurred. The motion is completely unsatisfactory with δ and $\dot{\delta}$ being limited most of the time.

The Velocity Command System

Linear analysis of the $n = 1$ system.- A linear analysis of the $n = 1$ system was made by using equation (7) subject to condition (10) to determine the effects of varying the gains K and K_1 and the servo time constant τ on the system response. A step input of $\phi_i(t) = 60^\circ$ was used in this analysis.

The effect of varying K and K_1 is shown in figures 11(a) and 11(b) for $\tau = 0.01$ and 0.3 second, respectively. The effect of increasing K is to decrease the rise and response times for small values of K_1 at both values of τ. This effect is much less marked at high values of K_1. For combinations of K, K_1, and τ which result in oscillatory motions, that is, when $4KK_1\tau > (K + 1)^2$, increasing K adds damping to the system.

The most pronounced effect of increasing K_1 is to reduce the rise and response times. As can be seen from figure 2(b), the gain K_1 appears as a multiplicative factor on the bank-angle error, and thus the rolling-velocity command which controls the speed of response is directly proportional to K_1.

In order to improve the system response, K_1 should be increased to control the rise and response times while K is increased to add damping to the system. The servo time constant τ should be kept as small as possible.

REAC study of the $n = 1$ system.- The $n = 1$ system was studied on the REAC by using the nonwinding type of limiter and the exponential input.

With δ_l set at 20°, $\dot{\delta}_l$ was decreased from 100 deg/sec (fig. 12(a)) to 40 deg/sec (fig. 12(b)). This reduction in $\dot{\delta}_l$ causes the system to become more oscillatory, and the rise and response times are increased. A comparison of figures 12(a) and 12(c) shows the effect of reducing δ_l to 5° while $\dot{\delta}_l$ remains at 100 deg/sec. For this condition the δ motion closely approximates a square wave, and again

the third harmonic of the basic frequency of this wave appears in the ϕ and $\dot{\phi}$ motions. The rise time of the system is increased while the response time is almost unchanged. Reducing δ_l from 20° to 5° when $\dot{\delta}_l$ is 40 deg/sec (figs. 12(b) and 12(d)) produces results similar to those previously obtained. A comparison of figures 12(c) and 12(d) indicates that a reduction in $\dot{\delta}_l$ when δ_l is 5° does not appreciably affect the system response. The square-wave phenomenon and the insensitivity to reductions in $\dot{\delta}_l$ for $\delta_l = 5°$ were also noted in the displacement control system.

Linear analysis of the $n = 2$ system.- Equation (7) subject to condition (10) was used to make a linear analysis of the velocity control system for $n = 2$. A step input of $\phi_i(t) = 60°$ was used as the forcing function. As in the linear analysis of the $n = 1$ system, K, K_1, and τ were varied to determine their effect on the system response. Figure 13(a) shows the effect of increasing τ from 0.01 to 0.3 second on the system response. As τ is increased the system response becomes oscillatory, a condition that would be expected since the condition for neutral oscillatory stability is $\frac{1}{\tau} = K_1$. Thus for constant K_1 the severity of the oscillation increases directly with τ.

As K_1 is increased from 1.5 to 16 (fig. 13(b)), the system response becomes oscillatory. However, in spite of the oscillatory mode, both the rise time and response time show large decreases. The oscillations may be reduced or eliminated by increasing K. With $K_1 = 16$ increasing K to 64 gives a deadbeat response for the system and further decreases the rise and response times. The gains K and K_1 perform the same functions for this system as they did for the $n = 1$ velocity control system, K_1 controlling the speed of response and K the damping. However, in the $n = 2$ system, in order to minimize the oscillatory characteristics in the response, when τ is constant, K must be greater than K_1.

REAC investigation of the $n = 2$ system.- The $n = 2$ velocity control system was studied on the REAC with both types of limiters; a step input of $\phi_i(t) = 60°$ was used as a forcing function.

Two types of limiting were used for the $n = 2$ velocity control system, the nonwinding and winding types of limiters. These limiters have been discussed in a previous section of this paper.

When $\dot{\delta}$ is made unlimited by setting $\tau = 0$, the two types of limiters are equivalent. This condition is used to show the effect of limiting δ. Figures 14(a) and 14(b) show that, as δ_l is decreased from 20° to 10°, the smooth response of figure 14(a) is modified by an oscillatory mode. A decrease in δ_l to 5° (fig. 14(c)), causes this oscillation to become more severe.

The effect of reductions in $\dot{\delta}_l$ is shown for $\delta_l = 20^\circ$ in figures 15(a) and 15(b) and for $\delta_l = 5^\circ$ in 15(c) and 15(d) for the nonwinding type of limiter. For $\delta_l = 20^\circ$ a reduction in $\dot{\delta}_l$ from 100 deg/sec to 40 deg/sec causes oscillations to develop in the ϕ and $\dot{\phi}$ motions. When a similar reduction is made for $\delta_l = 5^\circ$, no appreciable change occurs in the motion. However, the square-wave condition at low values of δ_l noted for the preceding systems occurs in this case. The results for the winding type of limiter are shown in figures 16(a) and (b) for $\delta_l = 20^\circ$ and in figures 16(c) and 16(d) for $\delta_l = 10^\circ$. When $\dot{\delta}_l$ is reduced from 100 deg/sec to 40 deg/sec for $\delta_l = 20^\circ$, the oscillations occurring in the ϕ and $\dot{\phi}$ motions become more severe. When δ_l is 10°, a reduction of $\dot{\delta}_l$ from 100 deg/sec to 60 deg/sec causes the system to become unstable. No stable cases for $\delta_l = 5^\circ$ were found for the winding-type limiter. Until the system became unstable, the rise times varied very little, but, because of the oscillations, the response time was gradually increasing.

The Acceleration Control System

Linear analysis of the $n = 3$ system.- A linear analysis of $n = 3$ acceleration control system was made by using equation (8) subject to condition (11). The system constants that were varied during this investigation are K, K_1, K_2, and τ.

Figure 17 shows the effect of varying K on the ϕ response. As K is increased from 4 to 20, the oscillations and overshoot are eliminated. This increase in K is accompanied by an increase in rise time and a decrease in response time. The oscillations that occur for $K = 4$ would increase with decreasing K since for the values of K_1, K_2, and τ used the system is approaching the condition for neutral oscillatory stability, which occurs at $K = 1.55$.

As K_1 is increased from 0.75 to 2.0 (fig. 18), both the rise time and response time decrease. At $K_1 = 2.0$, an overshoot and slight oscillation occur in the response. Further increases in K_1 would cause this oscillation to become more severe.

As K_2 is increased from 3 to 6 (fig. 19), the ϕ response gradually flattens until at $K_2 = 6$ a visible change in slope occurs at $t = 0.8$ second. This change in slope is probably caused by a change in the damping introduced by the change in K_2 and the limits placed on the velocity and acceleration commands because of the way in which they are determined. With $K_2 = 6$, increasing K_1 to 2 improves the system response and decreases the rise and response times. The increase in K_1 has decreased the system damping and liberalized the limits on the velocity and acceleration commands.

As τ is increased from 0.1 to 0.2 second (see fig. 20), the ϕ response is practically the same up to some point between $\tau = 0.1$ to 0.2 second. At this point an oscillation starts to develop, which is quite evident at $\tau = 0.2$ second (see dashed curve in fig. 20). As τ is further increased, this oscillation will become more severe until, at $\tau = 0.3$ second, neutral stability occurs (see eq. (8) and conditions for unstable operation).

A study of figures 17, 18, and 19 indicates that K controls the damping, while K_2 controls the rapidity of the initial response and affects the damping. The gain K_1 exerts an influence on the rise and response times that is inversely proportional to magnitude. Thus, increases in K_1 and K_2 will improve the speed of response and increasing K together with the increase in K_2 keeps the system response nonoscillatory and should give a better overall system response. Accordingly, K_1 was increased to 3.25, K_2 to 10, and K to 20 while τ was held constant. This response, shown in figure 21, is deadbeat with much smaller rise and response times than have previously been obtained for the $n = 3$ acceleration control system.

REAC investigation of the $n = 3$ system.- A step input of $\phi_i(t) = 60^\circ$ was used as the forcing function in the REAC study of the $n = 3$ acceleration control system. A winding-type limiter was used for this system. Since the winding-type limiter gives a more conservative result for a given system than the nonwinding type of limiter, the trends for the $n = 3$ system as studied should also indicate the trends to be expected if the nonwinding limiter had been used. The major difference between the effect of the two types of limiters is that regions of unstable operation indicated for the system with the winding-type limiter might not occur under similar conditions for a system equipped with the nonwinding limiter.

The effect of limiting δ and $\dot{\delta}$: In order to show the effect of reducing δ_l on the system response, the limit on the control-surface rate was removed by setting $\tau = 0$. As δ_l is reduced from 20° to 10° (figs. 22(a) and 22(b)), no apparent change occurs in the ϕ motion and a very slight oscillation is noted in the $\dot{\phi}$ and $\ddot{\phi}$ responses. When δ_l was reduced to 5°, the system became unstable.

With $\dot{\delta}_l$ set at 100 deg/sec and $\delta_l = 20^\circ$ (fig. 23(a)), a nonoscillatory response that is almost equivalent to the $\dot{\delta}_l = \infty$ response (fig. 22(a)) was obtained. Reducing $\dot{\delta}_l$ to 40 deg/sec (fig. 23(b)) introduces an extremely small oscillation into the ϕ, $\dot{\phi}$, and $\ddot{\phi}$ motions. Available results indicate that, for $\delta_l = 10^\circ$ and $\dot{\delta}_l = 100$ deg/sec and 40 deg/sec, the system response does not change appreciably from that shown in figure 23. When δ_l was reduced to 5°, unstable conditions were encountered for all values of $\dot{\delta}_l$.

Incomplete compensation: When the stability derivatives were varied individually or in a group, as indicated in table I, the $n = 3$ acceleration control system response was modified in the same way as the response of the displacement control system.

Changing the airframe flight condition from A to B (table I) produced unstable results for low values of K, thus following previous trends. However, when K was increased to 14 (fig. 24(a)), the instability was reduced to a hunting oscillation. Increasing K to 24 (fig. 24(b)) practically eliminated these oscillations in the ϕ response, and the oscillation in the other recorded variables is damped.

Remarks on other control systems using acceleration feedback.- Acceleration control systems described by equation (8) with $n = 1$ or 2, were superficially investigated by a linear analysis. The general trend of these reduced-order acceleration control systems was to require a different distribution of the forward-loop gain between K_1, K_2, and K than for the $n = 3$ system for the most satisfactory response. In addition, there are indications that higher values of the forward-loop gain can be used before limiting oscillations become severe enough to affect the system response adversely.

An acceleration control system with the $\dot{\phi}$ feedback eliminated and $K_2 = 1$ was investigated by linear methods. Routh's criterion indicated unstable conditions for $n > 1$. For $n = 1$ the system was stable for very small values of K and the allowable range of variation of K was small. The response of the system was very slow unless extremely large values of K_1 were used. These large values of K_1 commanded airplane accelerations that are considered as too high to be practical. Because of the high accelerations and the narrow band of K for stable operation, this system was not investigated on the REAC.

CONCLUDING REMARKS

The concept of the compensating network, a computing device that eliminates the dynamics of the controlled element from the system response, has been applied to automatic control systems. The general characteristics of this type of control system have been determined and the results applied to the analysis of three related automatic roll control systems for airplanes. These roll control systems differ in the number and type of feedbacks that are used to supply information to the compensating network for use in computing the control orders that produce cancellation of the airplane dynamics.

Within the limitations imposed by control-surface rate and displacement limiting and by imperfect compensation, the compensating network can give adequate command roll control that is free of airplane dynamic characteristics. Limiting of the control-surface rate and displacement introduces oscillatory modes into the system response that become more severe as the limiting time increases. Because of the way in which the limiting affects the system, restrictions were placed on the gains, the order of integration in the compensating network, and the servo time constant. The most critical effect caused by imperfect compensation occurs when a change in airplane flight condition, not accounted for by the compensating network, introduces an unstable response. Inaccuracies in the airplane mass and aerodynamic parameters used to design the network are not critical except in the case of C_{n_β} and C_{l_β} (partial derivatives of yawing-moment and rolling-moment coefficients with respect to sideslip angle) when hunting oscillations are introduced into the response. In addition to the difficulties introduced by limiting and incomplete compensation, the control of the yaw and sideslip motions are characteristically uncompensated in the command mode of operation.

The effects of limiting and imperfect compensation on the regulatory response are the same as for the command response.

Langley Aeronautical Laboratory,
National Advisory Committee for Aeronautics,
Langley Field, Va., May 12, 1955.

APPENDIX A

DEVELOPMENT OF TRANSFER FUNCTIONS FOR COMPENSATING-NETWORK CONTROL SYSTEMS

In this appendix the transfer functions of automatic control systems using compensating networks are developed. The transfer functions are derived for linear operating conditions and perfect compensation. The forward- and feedback-loop compensating network are discussed in the order mentioned.

The Forward-Loop Compensating Network

The block diagram of an airplane equipped with an automatic control system is shown in figure 1 where $F(D)$, $S(D)$, and $G(D)$ are the transfer functions of the compensating network, servo, and airplane, respectively.

An examination of the response characteristics of typical high-performance servos indicated that over the range of airplane frequencies a first-order time-lag servo was a good first approximation of a physical servo. Accordingly, the servo transfer function was taken as

$$S(D) = \frac{1}{1 + \tau D} \tag{A1}$$

where τ is the servo time constant. The closed-loop transfer function of the system is

$$\frac{X_o}{X_i} = \frac{F(D)\ S(D)\ G(D)}{1 + F(D)\ S(D)\ G(D)} \tag{A2}$$

It is desired to determine the transfer function of the compensating network $F(D)$ so that the airframe dynamics are canceled and that as a command system the closed-loop response has zero steady-state error. Basic servomechanism theory requires that, in a closed-loop system, an integration take place to satisfy the zero-steady-state-error condition (see ref. 5). Therefore, a logical choice for the compensating-network transfer function is

$$F(D) = \frac{K}{DG(D)} \tag{A3}$$

Substituting for $F(D)$ and $S(D)$ in equation (A2) results in the closed-loop transfer function

$$\frac{X_o}{X_i} = \frac{K}{\tau D^2 + D + K} \tag{A4}$$

and

$$\lim_{D \to 0} \frac{X_o}{X_i} = 1 \tag{A5}$$

Thus, the requirements that the airplane transfer is canceled and the steady-state error is zero are both satisfied. It should be noted that in compensating-network control systems the integration must always be introduced explicitly because implicit integration in the airplane transfer function is eliminated by the cancellation process.

In the foregoing analysis the transfer function $F(D)$ was determined to give complete compensation for a particular degree of freedom of the airplane X. If there is another degree of freedom η, which is related to X by the transfer function $G_1(D)$, (see fig. 1), η_o/X_i is given by

$$\frac{\eta_o}{X_i} = \frac{X_o}{X_i}\frac{\eta_o}{X_o} = \frac{X_o}{X_i} G_1(D) = \frac{K}{\tau D^2 + D + K} G_1(D) \tag{A6}$$

If $G_1(D)$ is the ratio of two polynomials, the output motion η_o will contain modes determined by the denominator of $G_1(D)$ since it appears as a factor of the characteristic equation of the system, and thus the response is uncompensated.

Behavior of the compensating-network control system as a regulator.- In addition to providing compensated control in response to command inputs, the control system is sometimes called upon to act as a regulator. If a disturbance $M(D)$ is applied to the airframe, as shown in figure 1, and the input $X_i \equiv 0$, the closed-loop transfer function is

$$\frac{X_o}{M} = \frac{G(D)}{1 + F(D)\ S(D)\ G(D)} \tag{A7}$$

Substituting $S(D) = \frac{1}{1 + \tau D}$ and $F(D) = \frac{K}{DG(D)}$ into equation (A7) yields

$$\frac{X_o}{M} = \frac{D(1 + \tau D)}{\tau D^2 + D + K} G(D) \tag{A8}$$

If $G(D)$ is the ratio of two polynomials in D and the denominator contains a constant, the steady-state condition for the regular response, $\lim_{D \to 0} \frac{X_o}{M} = 0$, is satisfied. However, $G(D)$ that appears in equation (A8) is a transfer function of the airplane. Since the denominator of $G(D)$ is a factor of the characteristic equation of the system, the response will contain airplane characteristics. Thus, the forward-loop compensating network does not eliminate airplane dynamics from the regulator response.

When the control system is responding to external disturbances (that is, when moments are applied to the airplane) the motion η_o is related to the disturbance M by the following transfer function:

$$\frac{\eta_o}{M} = \frac{X_o}{M} \frac{\eta_o}{X_o} = \frac{X_o}{M} G_1(D) = \frac{D(1 + \tau D)}{\tau D^2 + D + K} G(D)\, G_1(D) \tag{A9}$$

Thus, motions determined in part by the denominator of $G(D)$ will appear in the $\eta_o(D)$ motion. Thus, in most cases the response $\eta_o(D)$ will contain airplane modes and therefore the response is uncompensated.

The Feedback-Loop Compensating Network

Figure 25 is a block diagram of a simple displacement type of control system incorporating a feedback-loop compensating network. The transfer function of this control system for the command mode of operation, $X_i \neq 0$, $M = 0$, is

$$\frac{X_o}{X_i} = \frac{S_1(D)\, G(D)}{1 + F_1(D)\, S_1(D)\, G(D)} \tag{A10}$$

and for the regulatory mode of operation, $X_i = 0$, $M \neq 0$, the transfer function is

$$\frac{X_o}{M} = \frac{G(D)}{1 + F_1(D)\ S_1(D)\ G(D)} \tag{A11}$$

where $S_1(D)$, $G(D)$, and $F_1(D)$ are the transfer functions of the servo, airframe, and compensating network, respectively.

For the feedback-loop compensating-network control system, the servo transfer function assumed for this study is

$$S_1(D) = \frac{1}{D} S(D) = \frac{1}{D(1 + \tau D)} \tag{A12}$$

and if the transfer function of the compensating network is assumed to be

$$F_1(D) = \frac{R(D)\ S_1(D) - K\delta(D)}{KS_1(D)\ N(D)} \tag{A13}$$

the following system transfer functions result:

$$\frac{X_o}{X_i} = \frac{KN(D)}{R(D)} \tag{A14}$$

$$\frac{\eta_o}{X_i} = \frac{X_o}{X_i}\frac{\eta_o}{X_o} = \frac{KN(D)}{R(D)} G_1(D) \tag{A15}$$

for the command responses and

$$\frac{X_o}{M} = \frac{KD(1 + \tau D)\ N(D)}{R(D)} \tag{A16}$$

$$\frac{\eta_o}{M} = \frac{X_o}{M}\frac{\eta_o}{X_o} = \frac{KD(1 + \tau D)\ N(D)}{R(D)} G_1(D) \tag{A17}$$

for the regulatory responses.

In these transfer functions $R(D)$ is an arbitrary polynomial in D that defines the airplane response. If $R(D)$ is taken so that $(1 + \tau D)$ appears as a factor, the transfer functions for the regulatory response will become simpler.

Perfect compensation is present in contrast to the lack of compensation for some phases of operation found in the forward-loop compensating network obtained for all these responses. For equations (A14) and (A16) there are no airplane characteristics in the characteristic equation of the system. In equations (A15) and (A17) the denominator of $G_1(D)$, which is $N(D)$, is canceled by $N(D)$ in the numerator. In addition, equations (A14) to (A17) meet the required steady-state conditions for the command and regulatory responses.

It would appear that the feedback-loop compensating network is an ideal compensating system. However, there are two practical difficulties that arise with respect to this system. First, it appears that $R(D)$ must be a seventh-order polynomial in order to prevent derivatives from appearing in the system transfer function. Second, in the compensating network the numerator has a higher order than the denominator, which introduces derivatives into the system and the order of the derivative is such that it might make it very difficult to mechanize the compensating network. The use of a seventh-order polynomial for $R(D)$ would aggravate this condition.

Thus, before the feedback-loop compensating network can be evaluated, more basic research is required to determine whether the above-noted difficulties are inherent in the system.

APPENDIX B

THE INITIAL CONDITIONS IN THE COMPENSATING-NETWORK CONTROL SYSTEM

In the REAC study of the displacement control system, it was found that when a step input was used the response of the control, in the absence of control-surface rate and displacement limiting, was inconsistent with the results of the linear analysis for a similar input. Since servomechanism theory prescribes that, in order for a transfer function, as used in this paper, to exist, all initial conditions in the system must be zero (see ref. 5, p. 84), the characteristics of the step input and the equations of motion of the system were examined to determine if the assumption of zero initial conditions through the system had been violated on the REAC.

The step input was examined (see ref. 6) and it was found that for $t = 0$ the step input has an average mean value of $1/2$. This means that for the 60° step used the value of ϕ_i at $t = 0$ is 30°.

Figure 26 is a block diagram of the displacement control system as it was set up on the REAC. The equations of motion of this system are as follows:

$$\epsilon = \phi_i - \phi_o \tag{B1}$$

$$\epsilon_i = K\left(\phi_i - \phi_o\right) \tag{B2}$$

$$V_i = K\left(\phi_i - \phi_o\right) - X_o \tag{B3}$$

$$V_o = \mu g(D)\left[K\left(\phi_i - \phi_o\right) - X_o\right] \tag{B4}$$

$$\left(D - k_1\right)X_o - \left(k_2D^2 + k_3D\right)\xi - k_4\zeta = k_5V_o \tag{B5a}$$

$$-\left(k_6D + k_7\right)X_o + \left(D^2 - k_8D\right)\xi - k_9\zeta = 0 \tag{B5b}$$

$$-k_{10}X_o - k_{11}\int_0^t X_o - k_{12}D\xi + \left(D - k_{13}\right)\zeta = 0 \tag{B5c}$$

$$V_o = (1 + \tau D)\delta_a \tag{B6}$$

$$\left.\begin{aligned}
&\left(D^2 - k_1 D\right)\phi - \left(k_2 D^2 + k_3 D\right)\psi - k_4\beta = k_5\delta_a \\
&-\left(k_6 D^2 + k_7 D\right)\phi + \left(D^2 - k_8 D\right)\psi - k_9\beta = 0 \\
&-\left(k_{10} D + k_{11}\right)\phi - k_{12} D\psi + \left(D - k_{13}\right)\beta = 0
\end{aligned}\right\} \tag{B7}$$

where k_1 to k_{13} are functions of the airplane mass and aerodynamic parameters, ϵ, ϵ_i, and V_o are defined in figure 26, and X_o, ξ, and ζ correspond to ϕ, ψ, and β, respectively. The transfer function of the high-gain amplifier is $g(D)$ and μ is the gain of this amplifier.

After assuming the transfer function of the high-gain amplifier $g(D)$ to be unity and taking account of the initial condition on ϕ_i, the determinant of the equations of motion was expanded for $\phi_o(D)$. This expansion gave

$$\phi_o = \frac{-f_1(D)\left\{\mu K\left[\frac{1}{D} f_2(D) + \mu f_1(D)\right] - \mu^2 K f_1(D)\right\}\phi_i}{f_2(D)\left\{-(1 + \tau D)\left[\frac{1}{D} f_2(D) + \mu f_1(D)\right]\right\} - f_1(D)\left\{\mu K\left[\frac{1}{D} f_2(D) + \mu f_1(D)\right] - \mu^2 K f_1(D)\right\}} +$$

$$\frac{-\mu f_1(D)\left\{\left[-\left(k_2 D - k_3\right)\left(D - k_{14}\right) - k_4 k_{12}\right] k_6 + \frac{1}{k_5} f_1(D)\right\} X_o(0)}{f_2(D)\left\{-(1 + \tau D)\left[\frac{1}{D} f_2(D) + \mu f_1(D)\right]\right\} - f_1(D)\left\{\mu K\left[\frac{1}{D} f_2(D) + \mu f_1(D)\right] - \mu^2 K f_1(D)\right\}} \tag{B8}$$

and

$$\lim_{\mu \to \infty} \phi_o = \frac{k\phi_i}{\tau D^2 + D + K} + \frac{\left\{\left[-\left(k_2 D - k_3\right)\left(D - k_{14}\right) - k_4 k_{12}\right] k_6 + \frac{1}{k_5} f_1(D)\right\} X_o(0)}{\left(\tau D^2 + D + K\right) f_2(D)} \tag{B9}$$

In this equation $f_1(D)$ is the numerator of the transfer function ϕ/δ_a and $f_2(D)$ is the denominator of that transfer function.

The first term on the right-hand side, after being divided by ϕ_i, is easily recognizable as the transfer function for ϕ_o/ϕ_i used in the linear analysis. The second term is a function of the initial value of X_o. If $X_o(0) \equiv 0$, this term is zero and complete compensation takes place. If $X_o(0) \neq 0$, this term is not zero and complete compensation does not occur. By evaluating equations (B1) to (B5) at $t = 0$, it can be shown that

$$X_o(0) = K\phi_i(0) \tag{B10}$$

Thus, if a step input is used, complete compensation will not take place. However, if $\phi_i(t) = \phi_c(1 - e^{-at})$, then $\phi_i(0) \equiv 0$ and from equation (B10) $X_o(0) \equiv 0$; thus the second term on the right-hand side of equation (B9) becomes zero and complete compensation takes place.

This analysis was extended to cover the velocity and acceleration control systems. For these systems it was found that when $n = 1$ the exponential input had to be used to get complete compensation. For $n > 1$ the step input could be used and complete compensation was obtained.

REFERENCES

1. Owen, J. C.: Report on Automatic Pilot for High Performance Aircraft. U. S. A. F. Exhibit MCREXE11-133, Contract AF-33(038)5700. Rep. No. 8, Eclipse-Pioneer Div. of Bendix Aviation Corp., Sept.-Oct. 1950, pp. 35-50.

2. Truxal, John, Smead, Joseph, and Clauser, Milton: Mechanical Compensation of Aircraft Longitudinal Control Systems. Rep. No. A-53-1 (Contract N7onr 39414), Purdue Univ., Mar. 1953. (Available as AD No. 20072 from Armed Services Tech. Information Agency, Document Service Center (Dayton, Ohio).)

3. Andrews, E. J.: Automatic Control and the Airplane. BUAER Rep. AE-61-5 Pt. II, Report of the Second Piloted Aircraft Flight Control Symposium, June 2-5, 1952, pp. 41-60.

4. Sternfield, Leonard: Several Factors Affecting Roll Control Systems of Interceptors. NACA RM L53I22a, 1953.

5. Brown, Gordon S., and Campbell, Donald P.: Principles of Servomechanisms. John Wiley & Sons, Inc., 1948, chs. 2 and 6.

6. Jeffreys, Harold, and Jeffreys, Bertha Swirles: Methods of Mathematical Physics. Cambridge Univ. Press, 1946.

TABLE I.- AIRPLANE FLIGHT CONDITIONS AND CHARACTERISTICS CONSIDERED

Parameter	Flight condition			
	A (standard)	A-1 (singular variations)	A-2 (group variations)	B
H, ft	60,000			60,000
ρ, slugs/cu ft	0.000224			0.000224
W, lb	26,547			26,547
b, ft	35.81			35.81
S, sq ft	401			401
V, ft/sec	1,942			1,359
ϵ, deg	6.95			0
α, deg	3.58			5.04
$\eta = \epsilon + \alpha$, deg	10.53			5.04
μ	256			
K_x^2	0.0151			0.0124
K_z^2	0.113			0.116
K_{xz}	0.0188			0.00916
b/v	0.01844			0.02635
M	2.0			1.4
C_{L_α}	0.044			0.0635
C_L	0.157			0.320
$C_{l_{\delta_\alpha}}$	-0.0773			-0.117
C_{l_p}	-0.205	-0.15,-0.25	-0.15	-0.275
C_{l_β}	-0.106	-0.08,-0.13	-0.13	-0.128
C_{l_r}	0.158	0.12,0.2	0.12	0.189
C_{n_p}	0.0275	-0.01,0.05	-0.01	-0.014
C_{n_β}	0.285	0.25,0.32	0.32	0.345
C_{n_r}	-0.600	-0.5,-0.7	-.500	-0.690
C_{Y_β}	-0.695	-0.6,-0.8	-0.600	-0.785

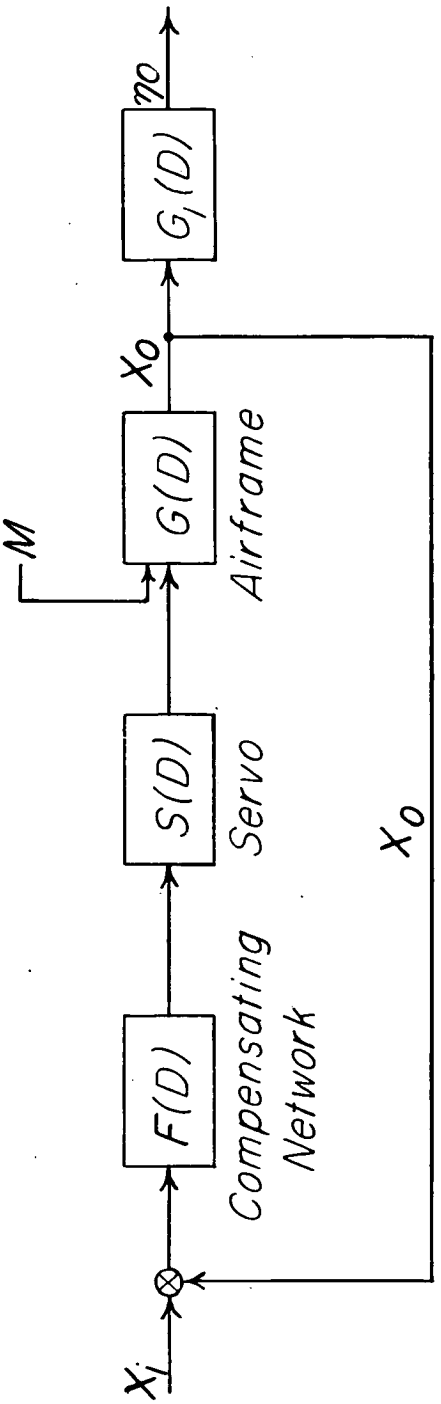

Figure 1.- Block diagram of generalized automatic control system incorporating a compensating network.

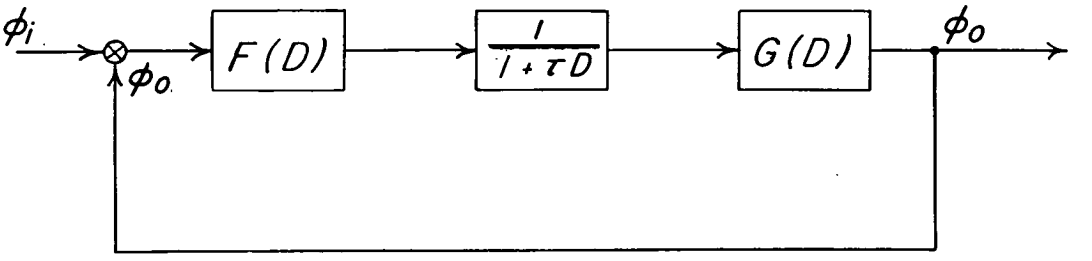

(a) Displacement control system.

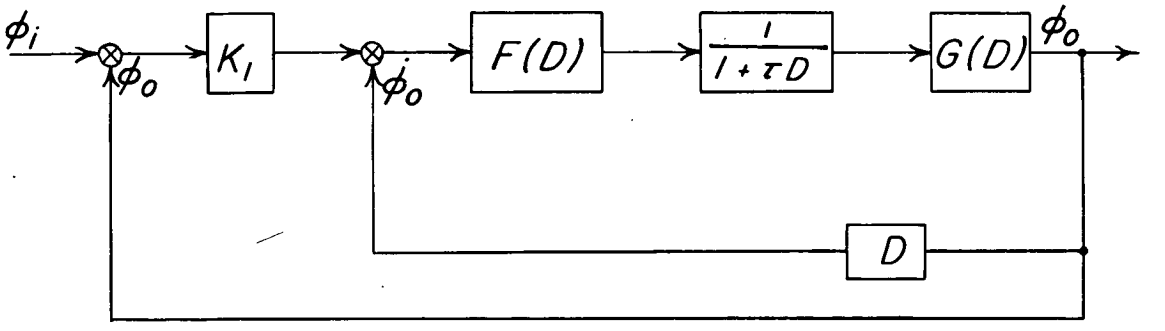

(b) Velocity control system.

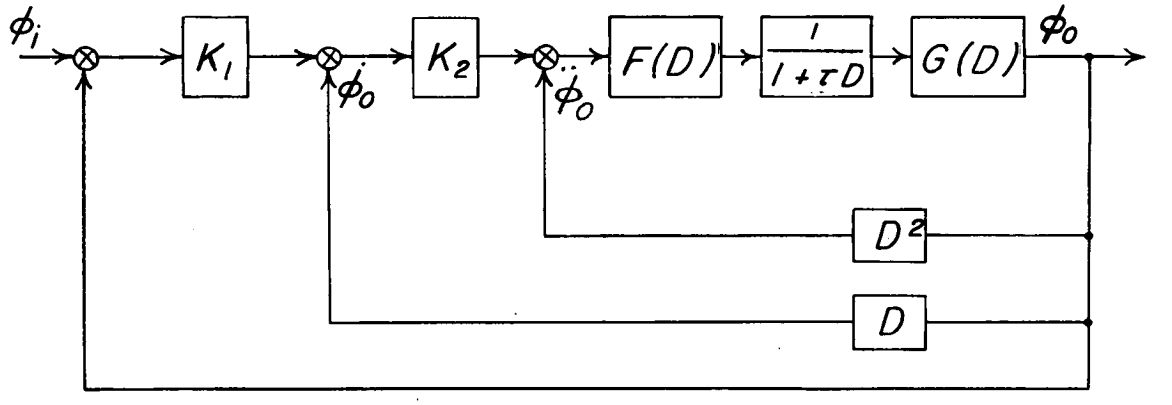

(c) Acceleration control system.

Figure 2.- Block diagrams of roll control systems incorporating a compensatory network.

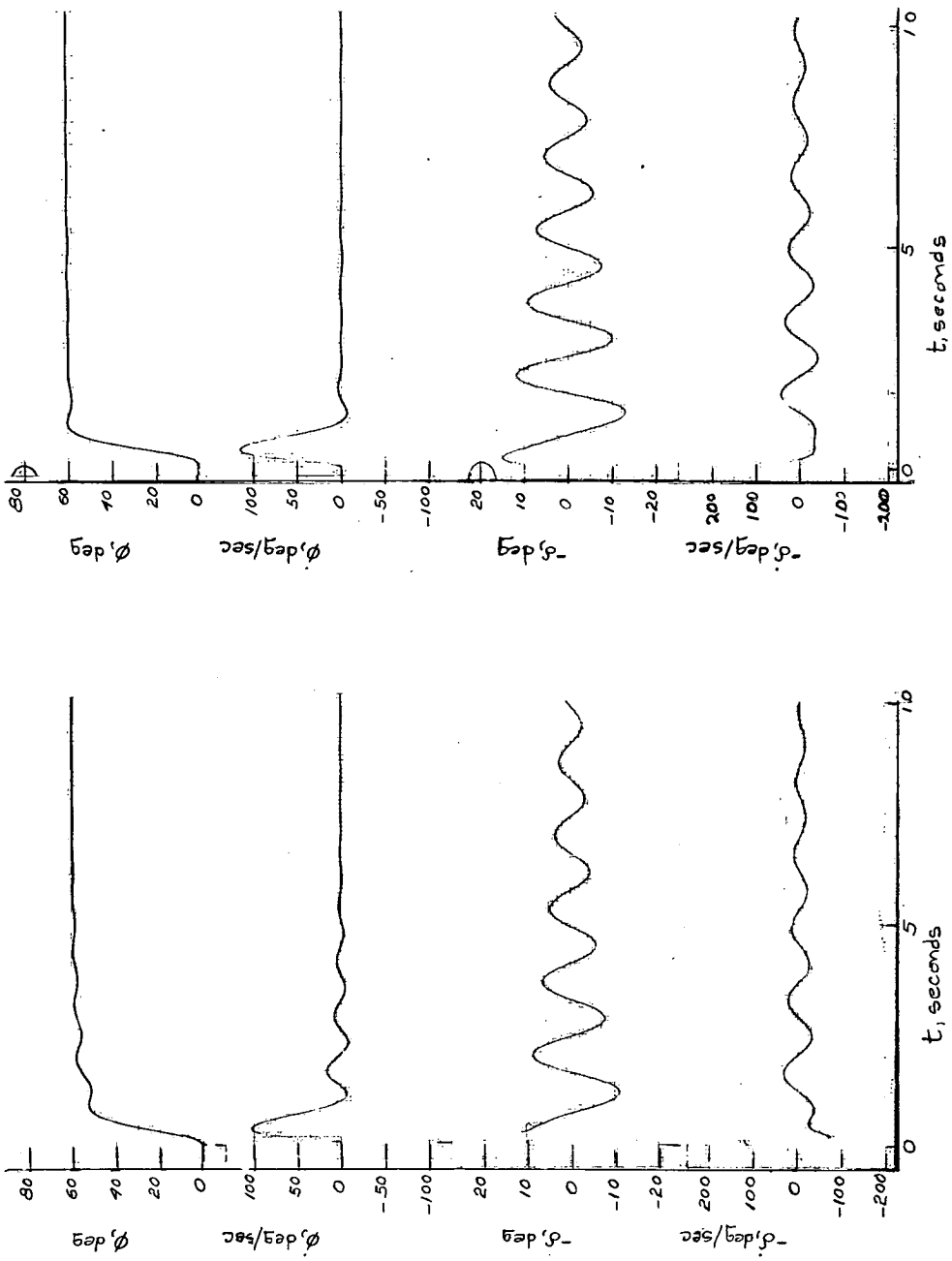

Figure 3.- Effect of τ on the response of the displacement control system. K = 5; δ_l = 20°; δ_l = 100 deg/sec; flight condition A; exponential input a = 4.

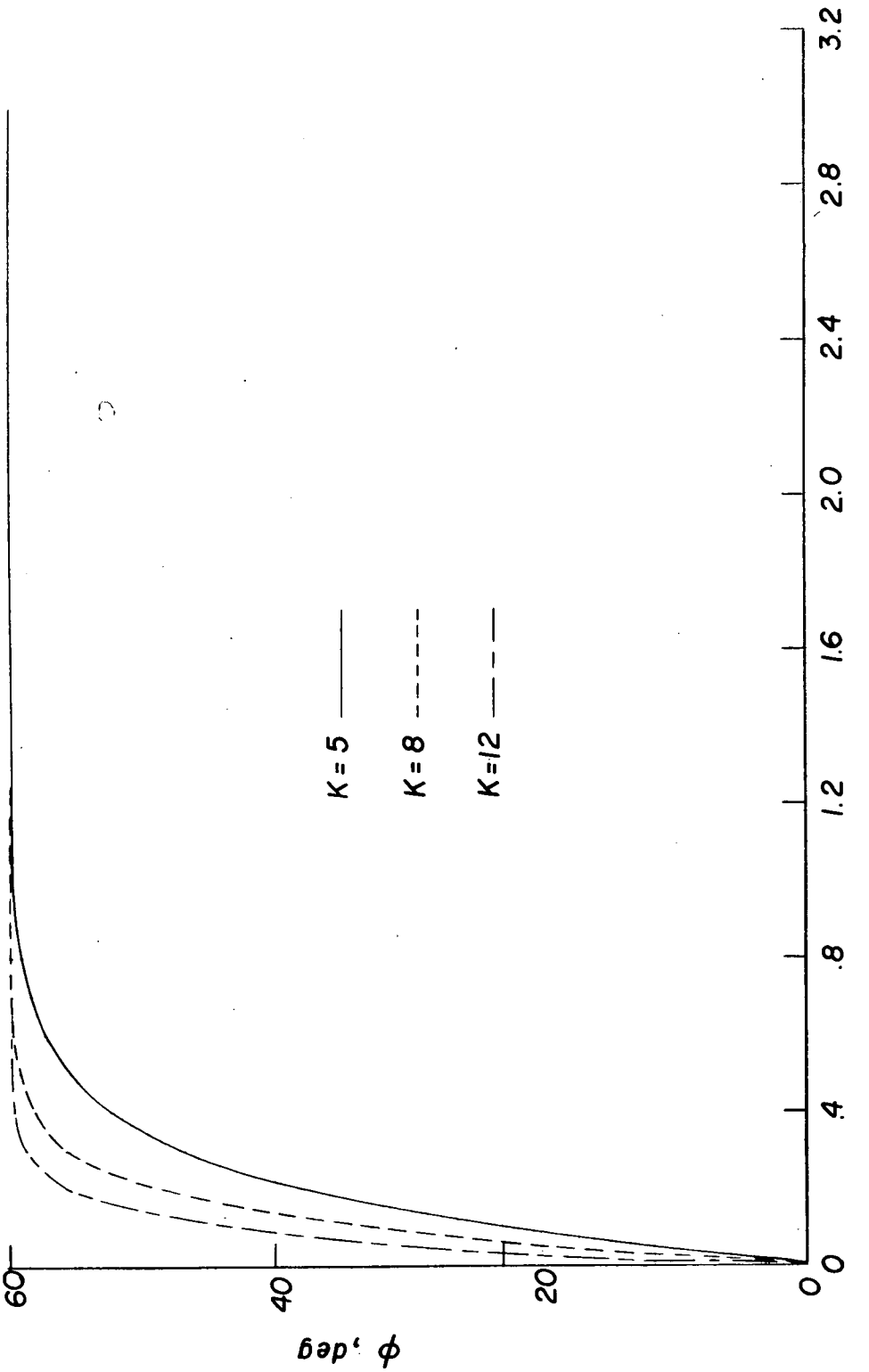

Figure 4.- ϕ response of the displacement control system for various values of K. τ = 0.01 second; flight condition A.

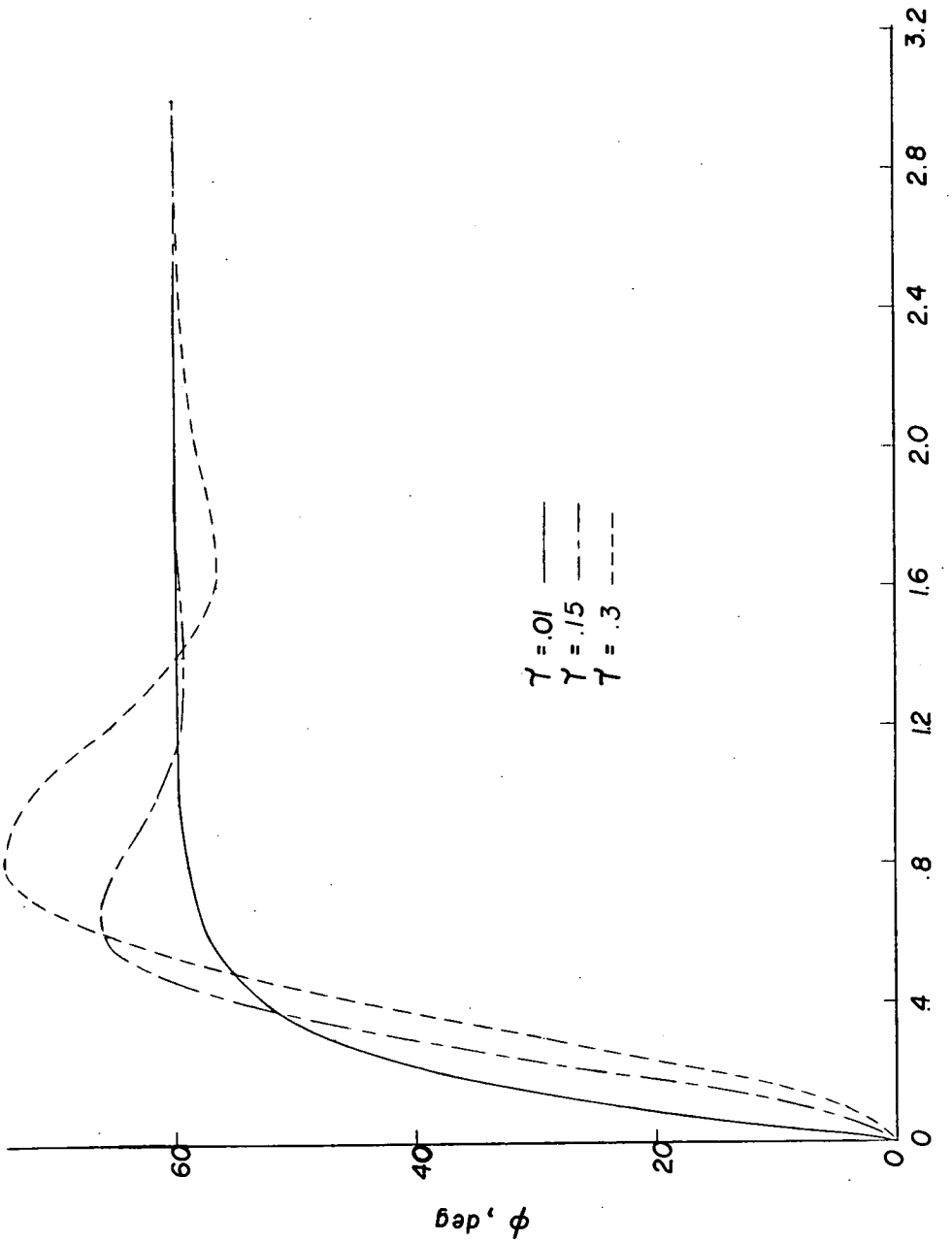

Figure 5.- ϕ response of the displacement control system for various values of τ. K = 5; flight condition A.

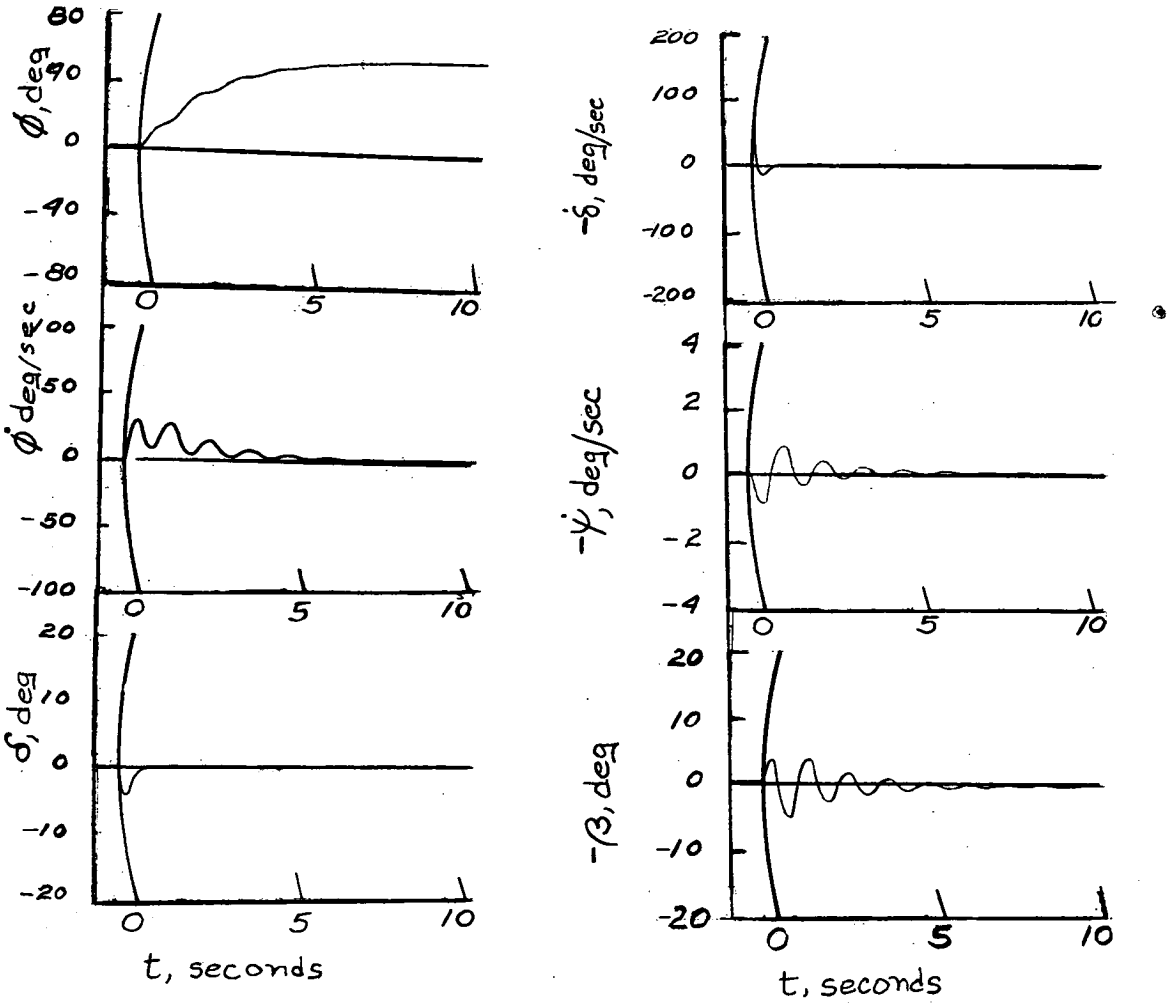

(a) REAC result for step input $\phi_i = 60°$.

Figure 6.- Response of displacement control system. K = 5; τ = 0.1 second; flight condition A; no limiting.

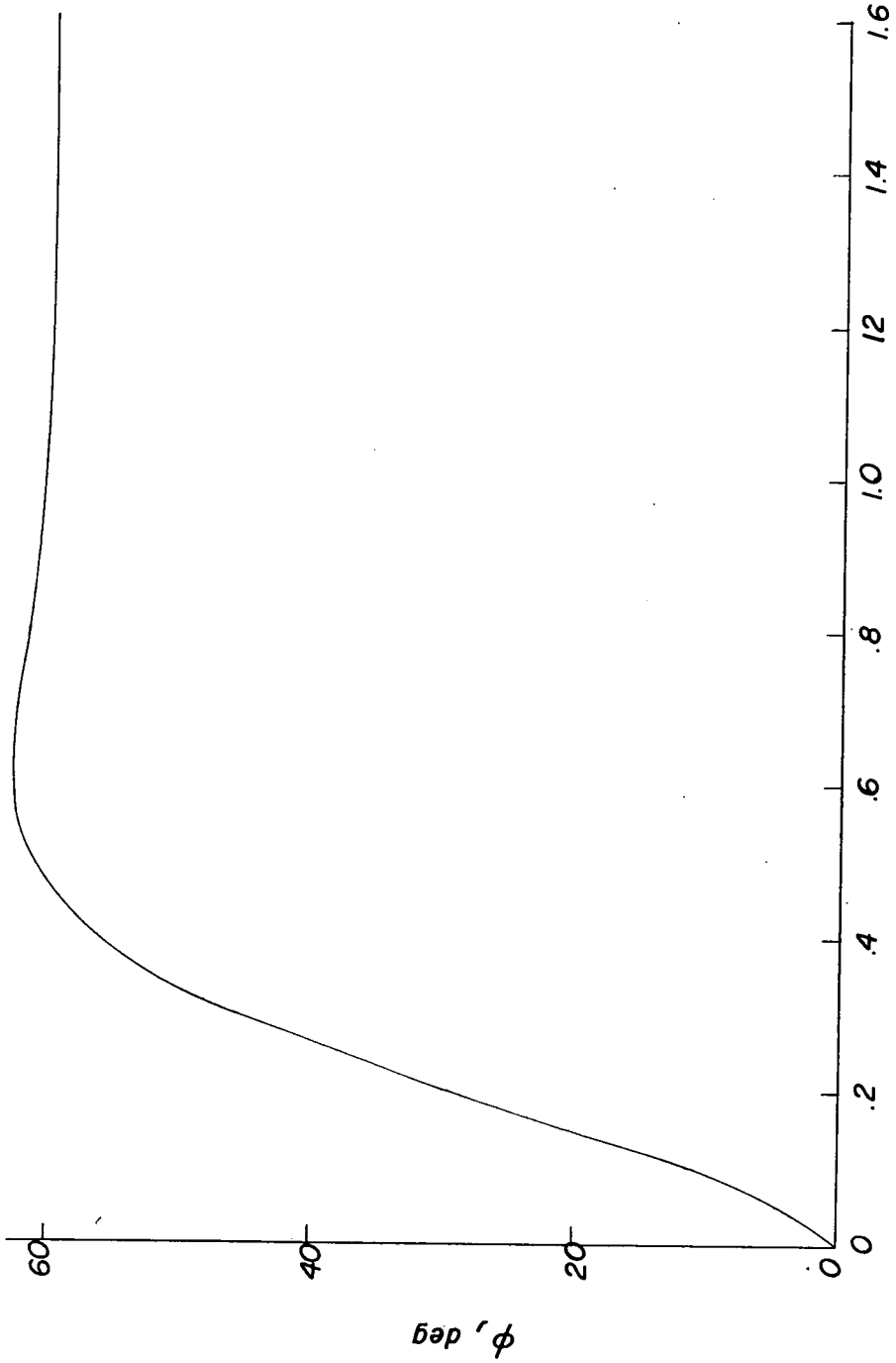

(b) Linear result.

Figure 6.- Concluded.

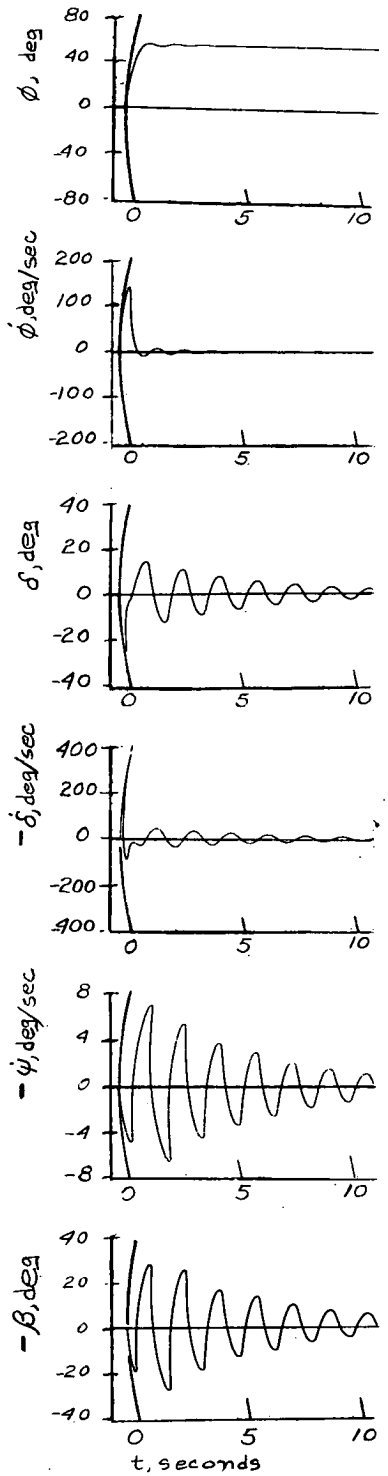

Figure 7.- Response of displacement control system. K = 5; τ = 0.1 second; a = 8; flight condition A; exponential input $\phi_i = \phi_i(1 - e^{-at})$; no limiting.

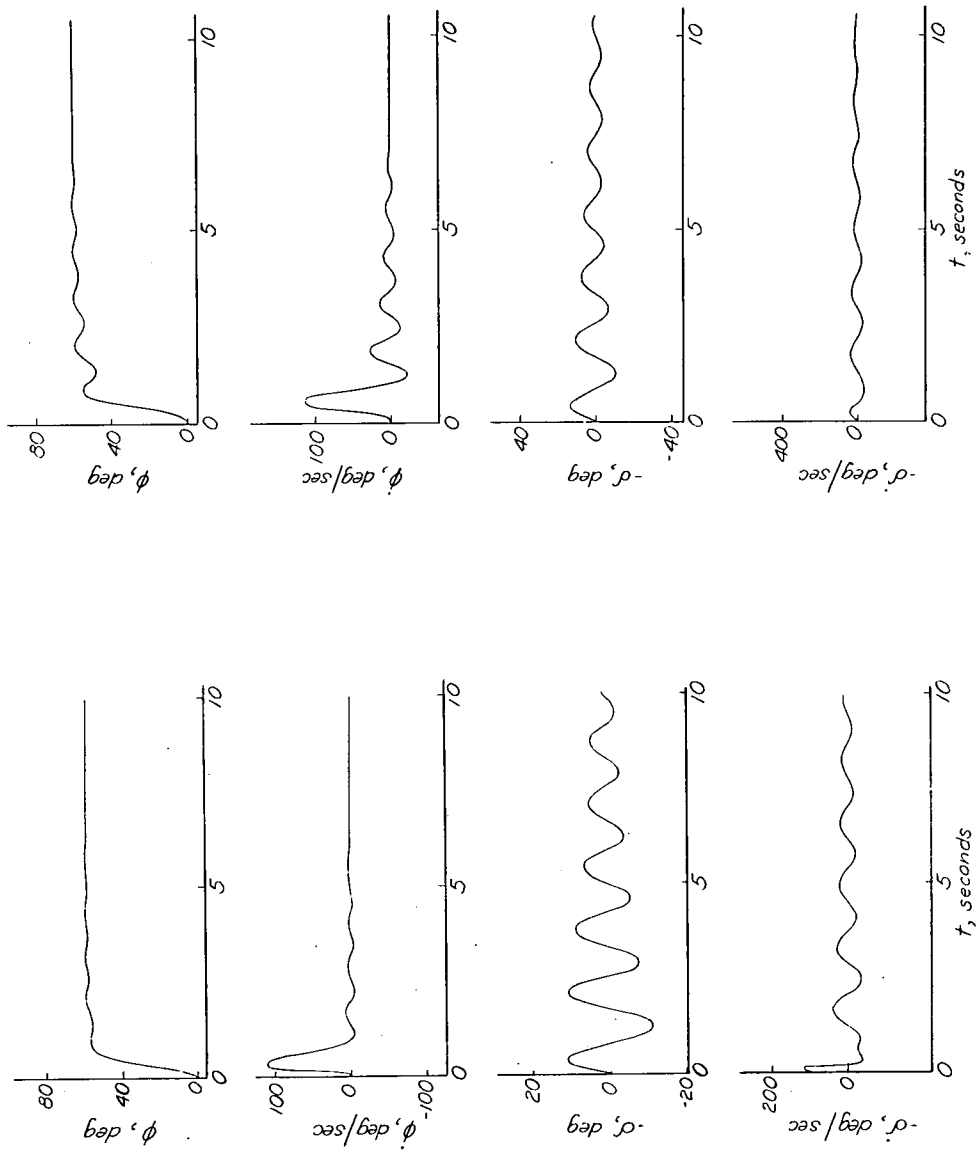

(a) $\delta_l = 20°$; $\dot{\delta}_l = 100$ deg/sec.

(b) $\delta_l = 20°$; $\dot{\delta}_l = 50$ deg/sec.

Figure 8.- Effect of limiting of $\dot{\delta}$ on the response of the displacement control system. K = 5; τ = 0.1 second; flight condition A; exponential input a = 4.

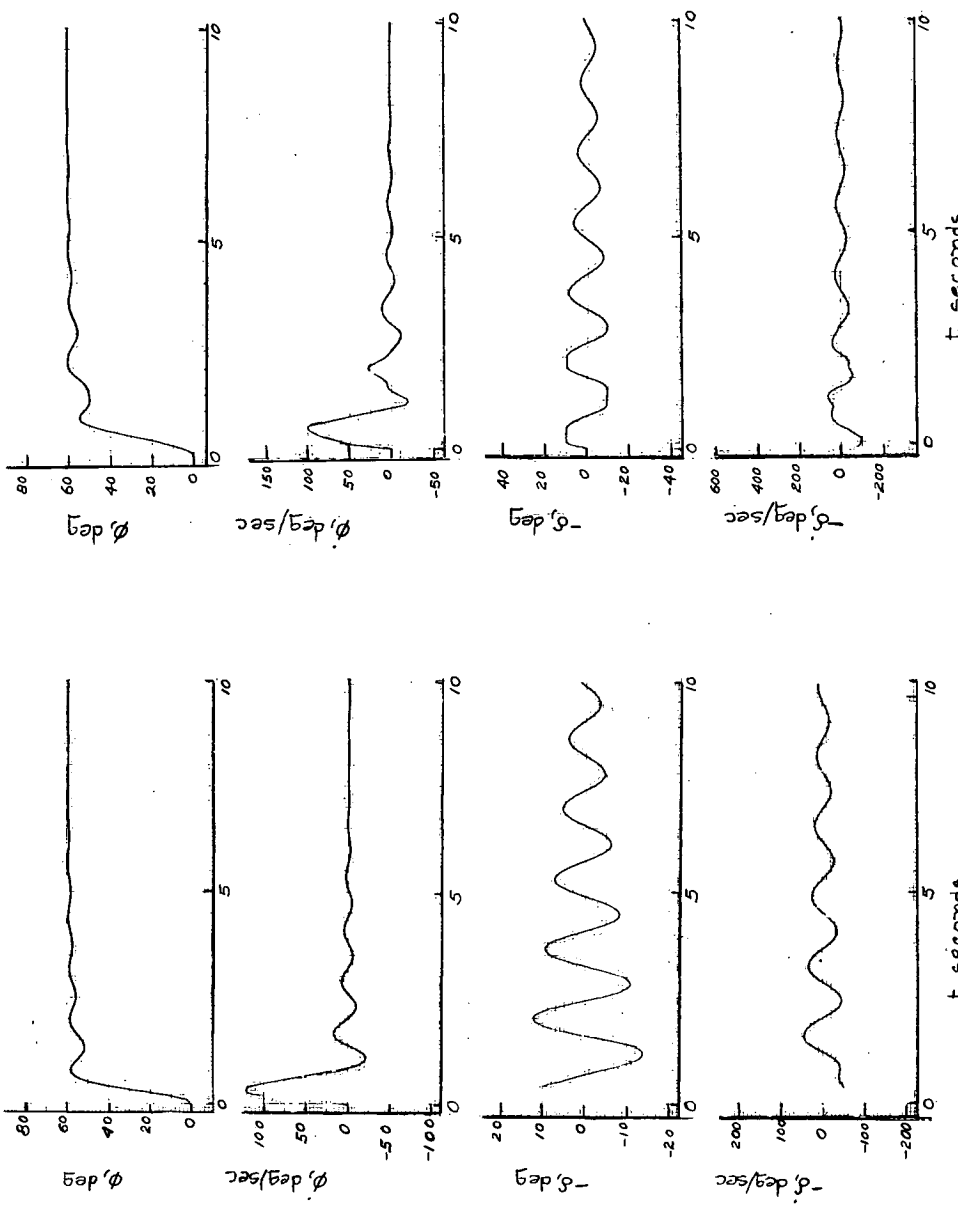

(a) $\delta_l = 20^\circ$; $\dot{\delta}_l = 100$ deg/sec.

(b) $\delta_l = 10^\circ$; $\dot{\delta}_l = 100$ deg/sec.

Figure 9.- Effect of limiting of δ on the response of the displacement control system. $K = 5$; $\tau = 0.1$ second; flight condition A; exponential input $a = 6$.

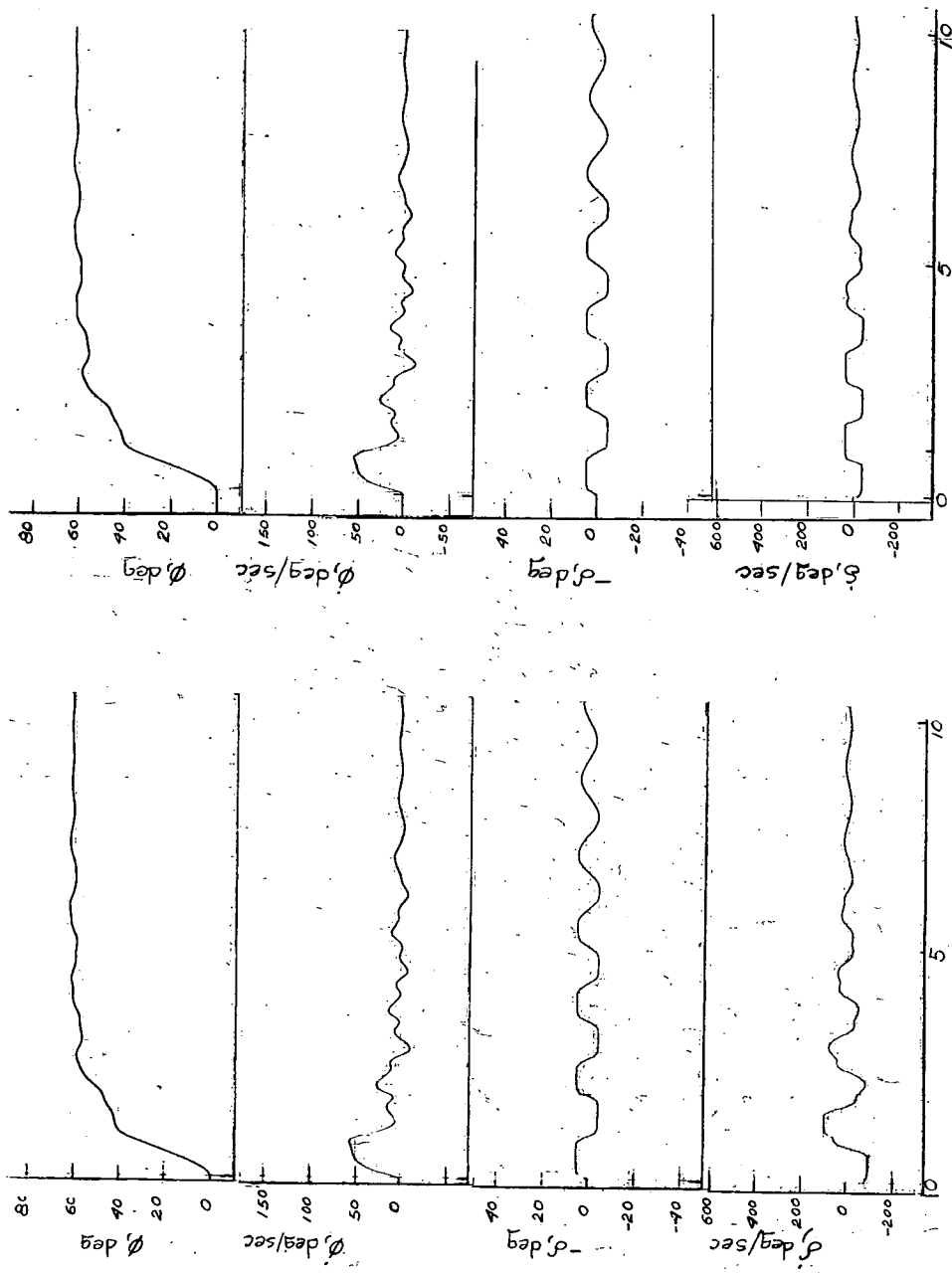

(c) $\delta_l = 5^\circ$; $\dot{\delta}_l = 100$ deg/sec.

(d) $\delta_l = 5^\circ$; $\dot{\delta}_l = 40$ deg/sec.

Figure 9.- Concluded.

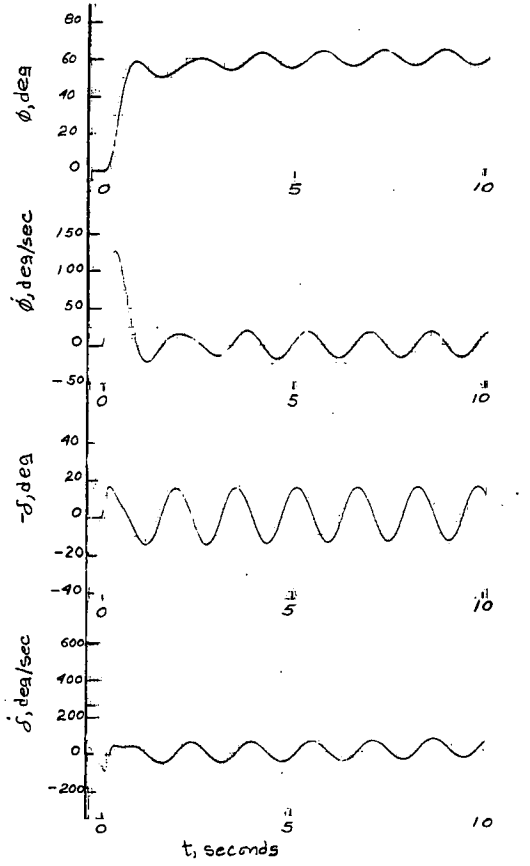

(a) C_{n_β} = 0.285 for compensating network; C_{n_β} = 0.32 for airframe; flight condition A.

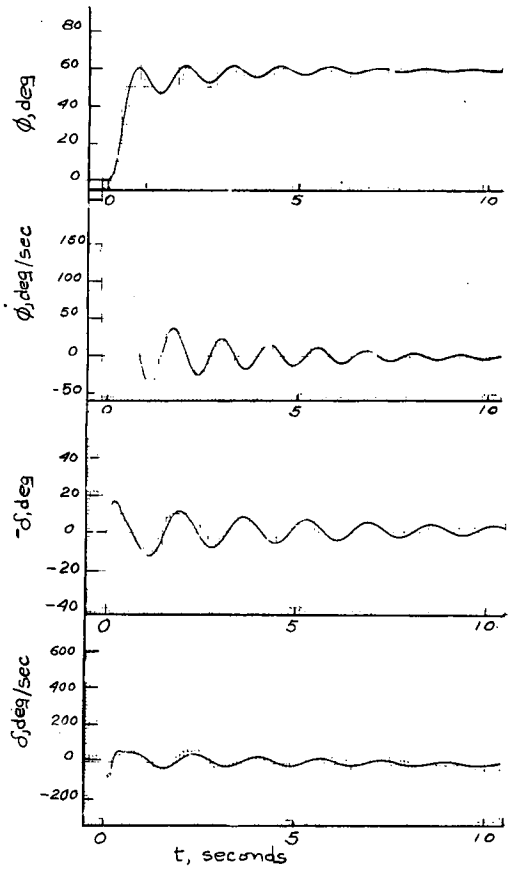

(b) C_{l_β} = -0.106 for compensating network; C_{l_β} = -0.08 for airframe; flight condition A.

Figure 10.- Effect of incomplete compensation on the response of the displacement control system. K = 5; τ = 0.1 second; exponential input a = 6; δ_l = 20°; $\dot{\delta}_l$ = 100 deg/sec.

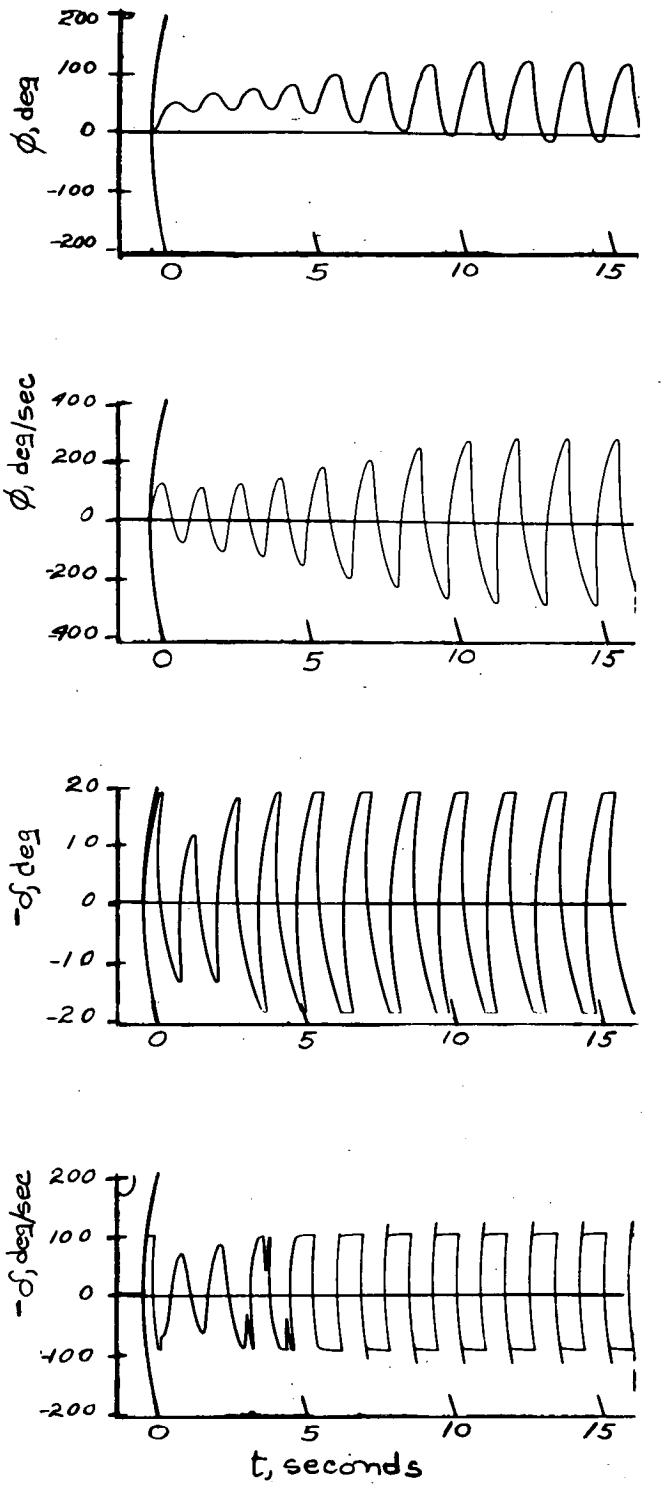

(c) Flight condition A in the compensating network and flight condition B in the airframe.

Figure 10.- Concluded.

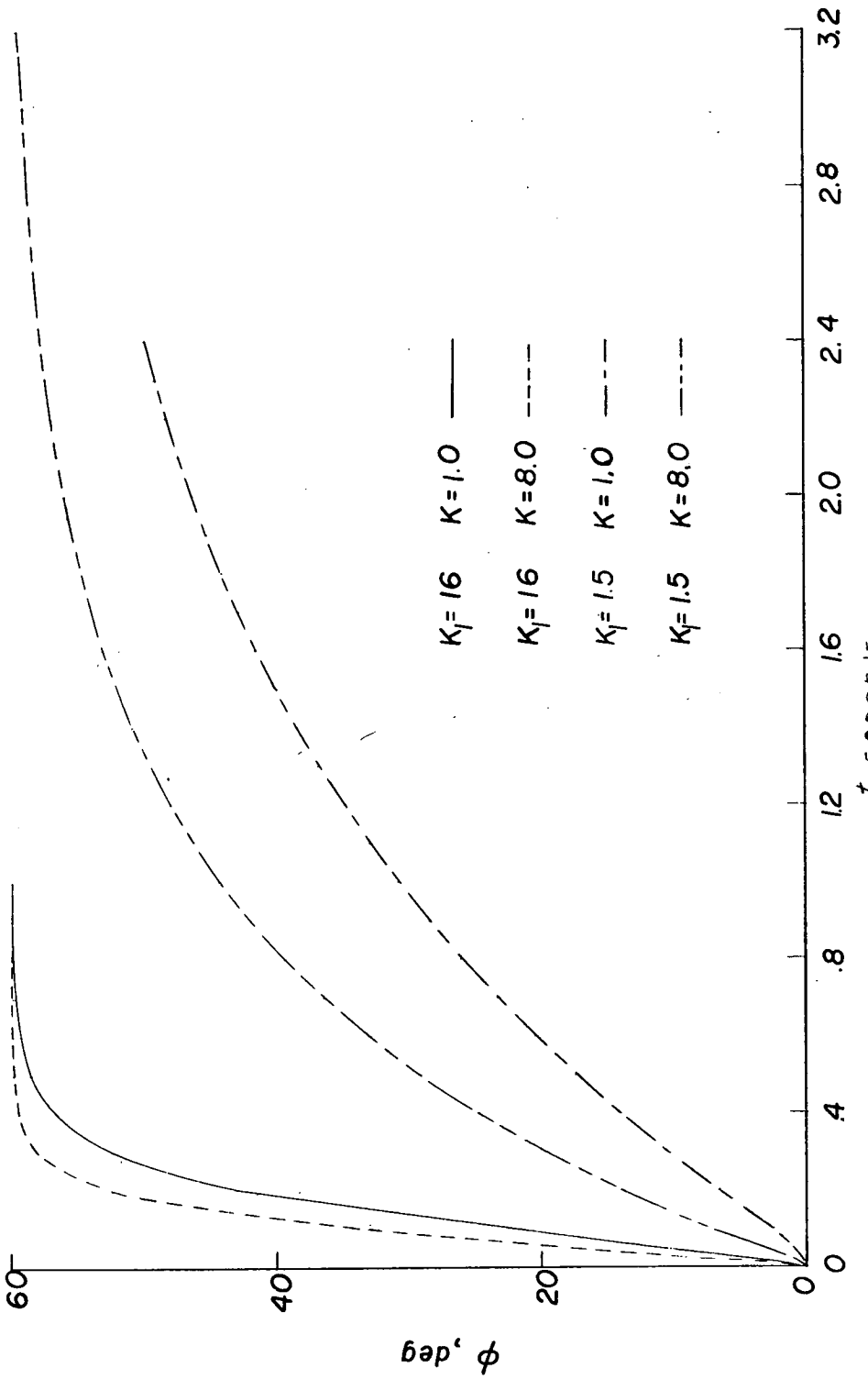

(a) τ = 0.01 second.

Figure 11.- ϕ response for the n = 1 velocity control system and various values of K and K_1. Flight condition A.

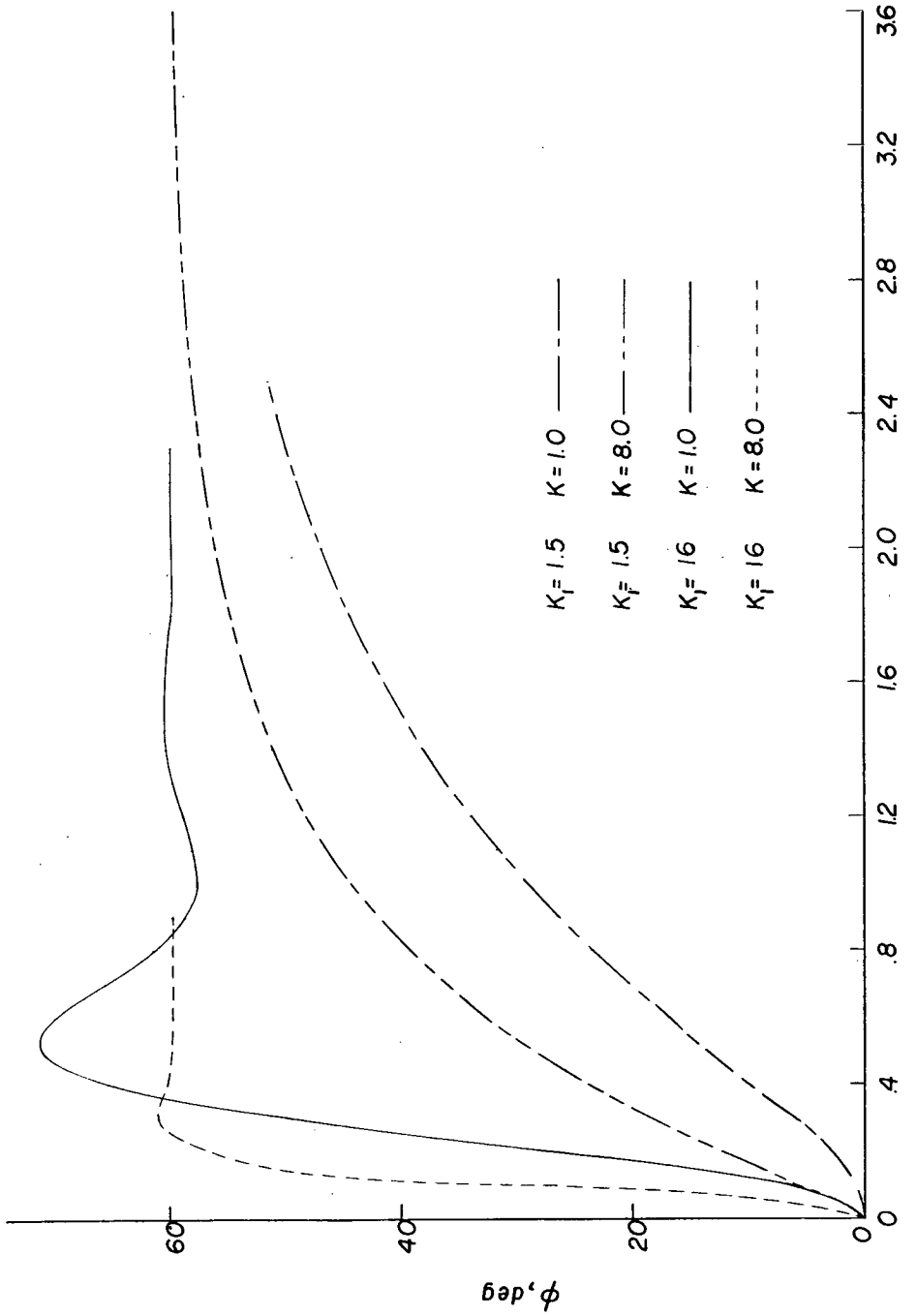

(b) τ = 0.3 second.

Figure 11.- Concluded.

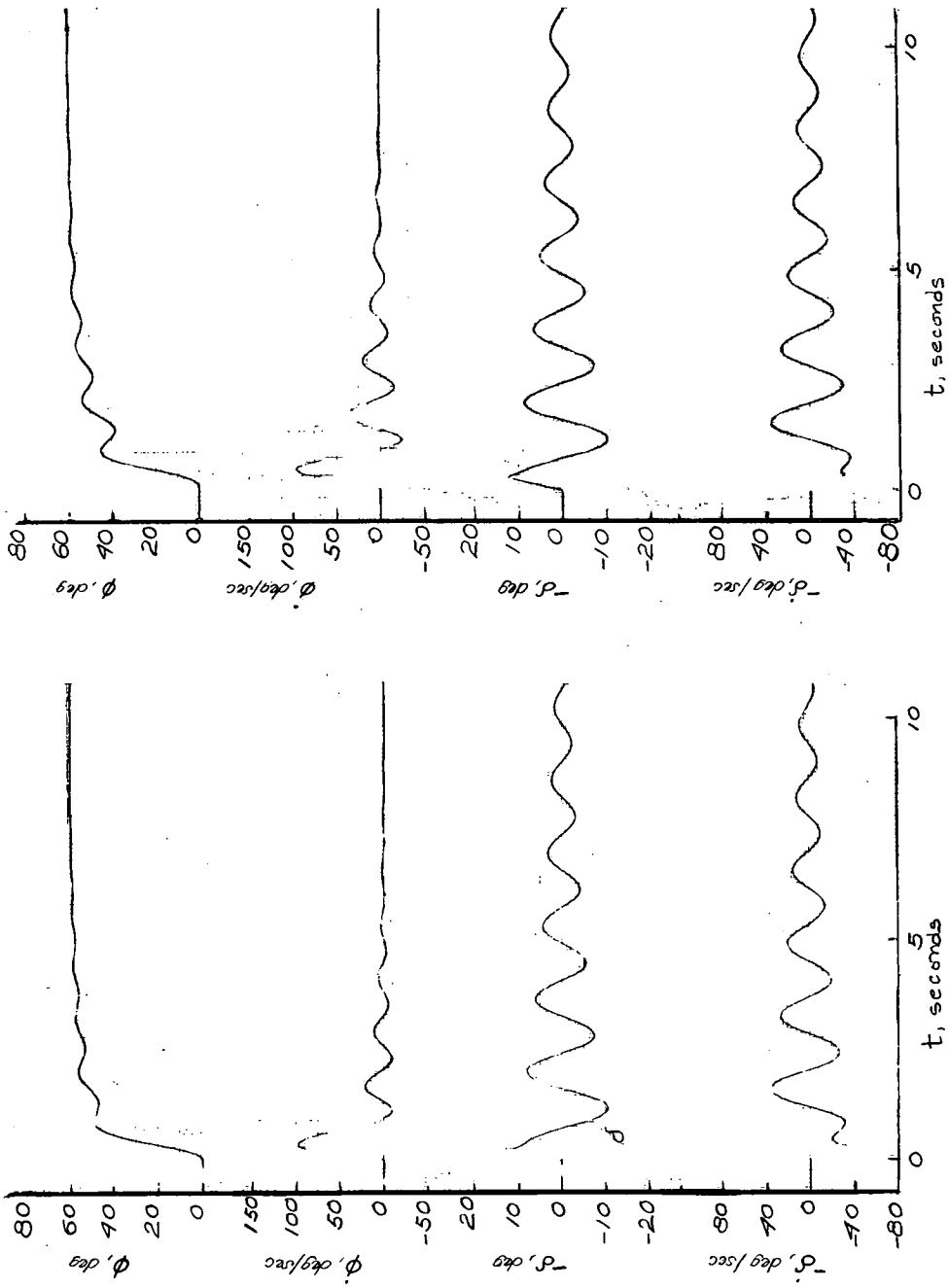

Figure 12.- Effect of limiting of δ and δ̇ on the response of the n = 1 velocity control system. K_1 = 4.0; K = 8.0; τ = 0.1 second; flight condition A; exponential input a = 6.

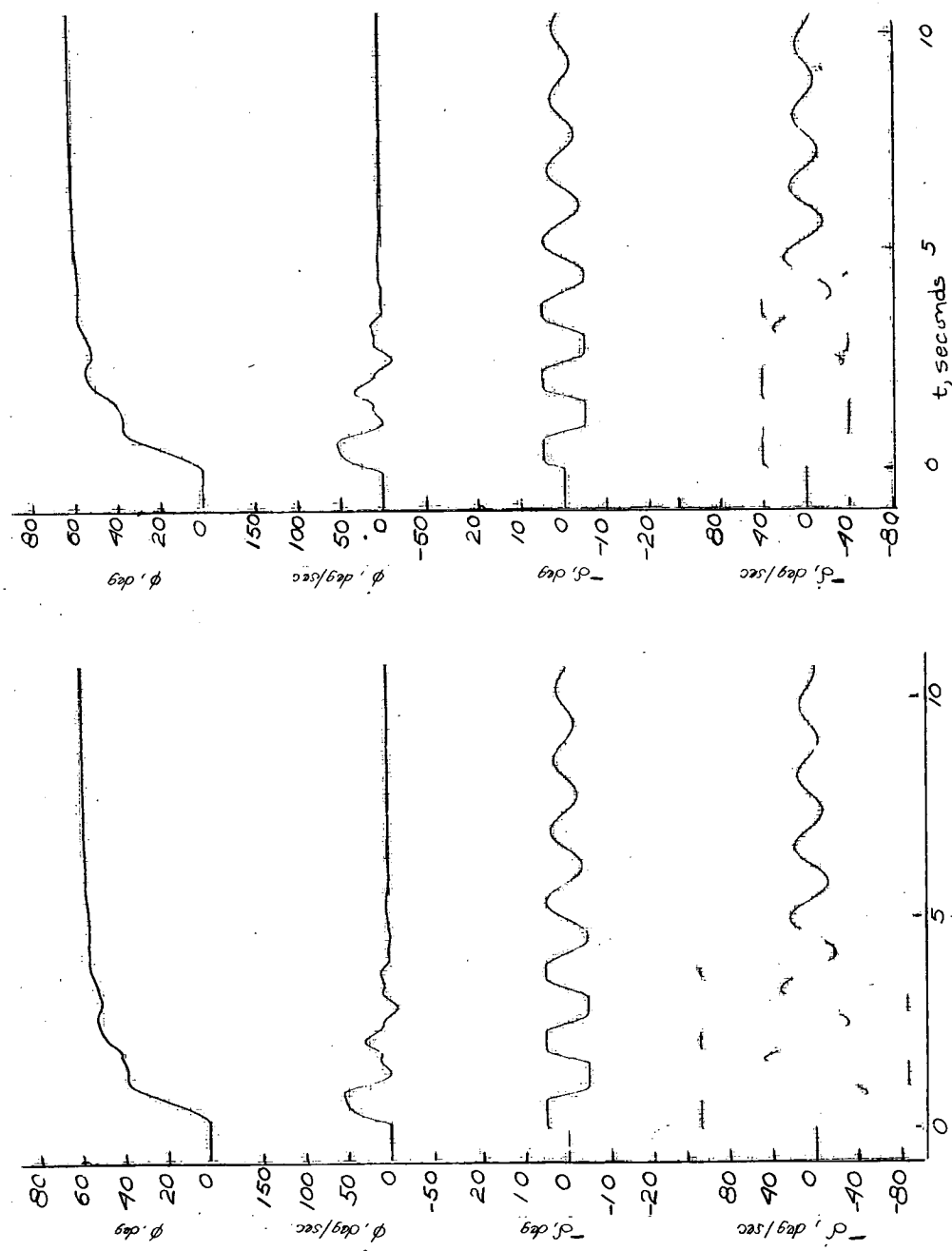

(c) $\delta_l = 5^\circ$; $\dot{\delta}_l = 100$ deg/sec.

(d) $\delta_l = 5^\circ$; $\dot{\delta}_l = 40$ deg/sec.

Figure 12.- Concluded.

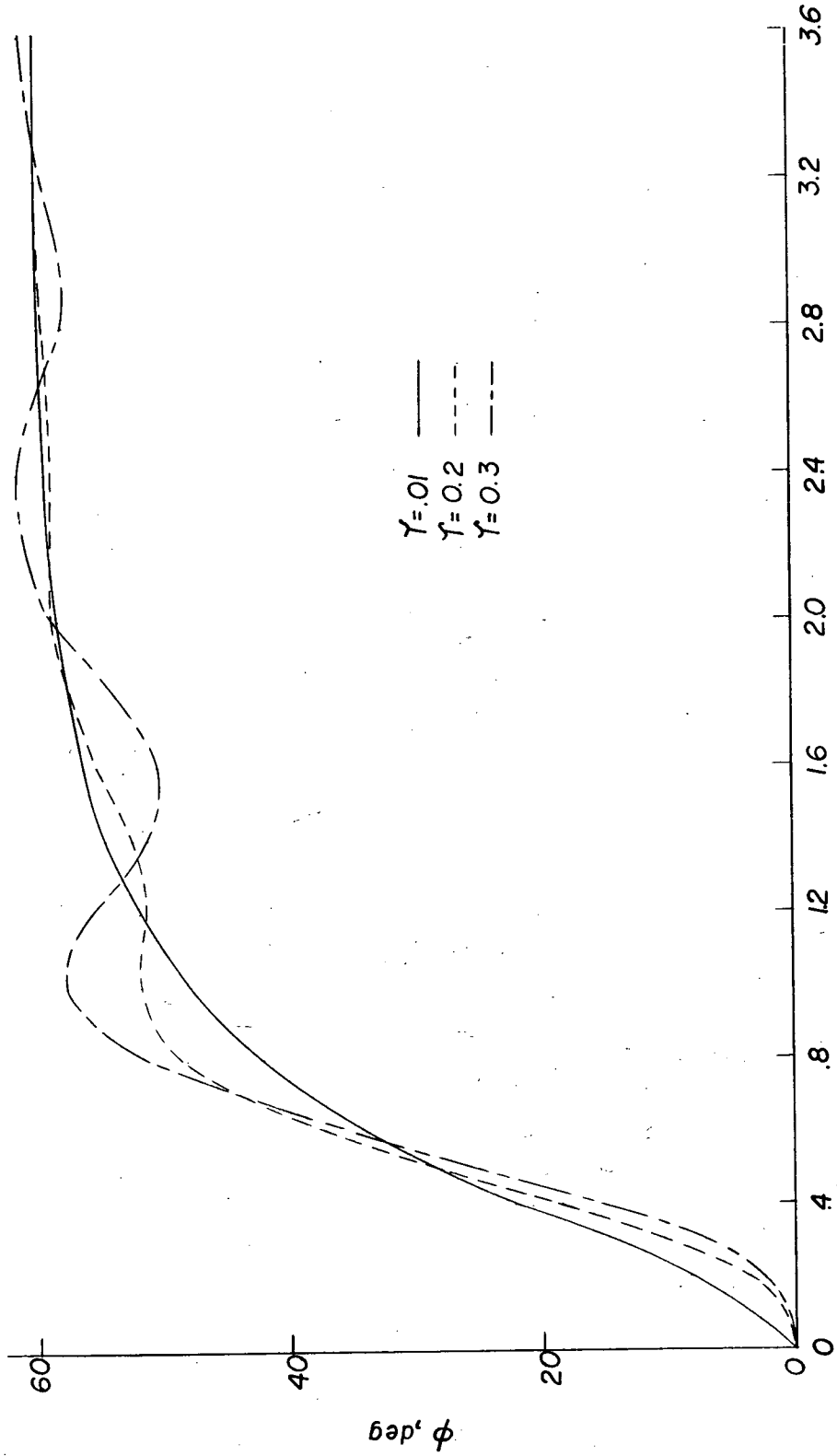

(a) The effect of τ for $K_1 = 1.5$, $K = 8$.

Figure 13.- ϕ response of the n = 2 velocity control system. Flight condition A.

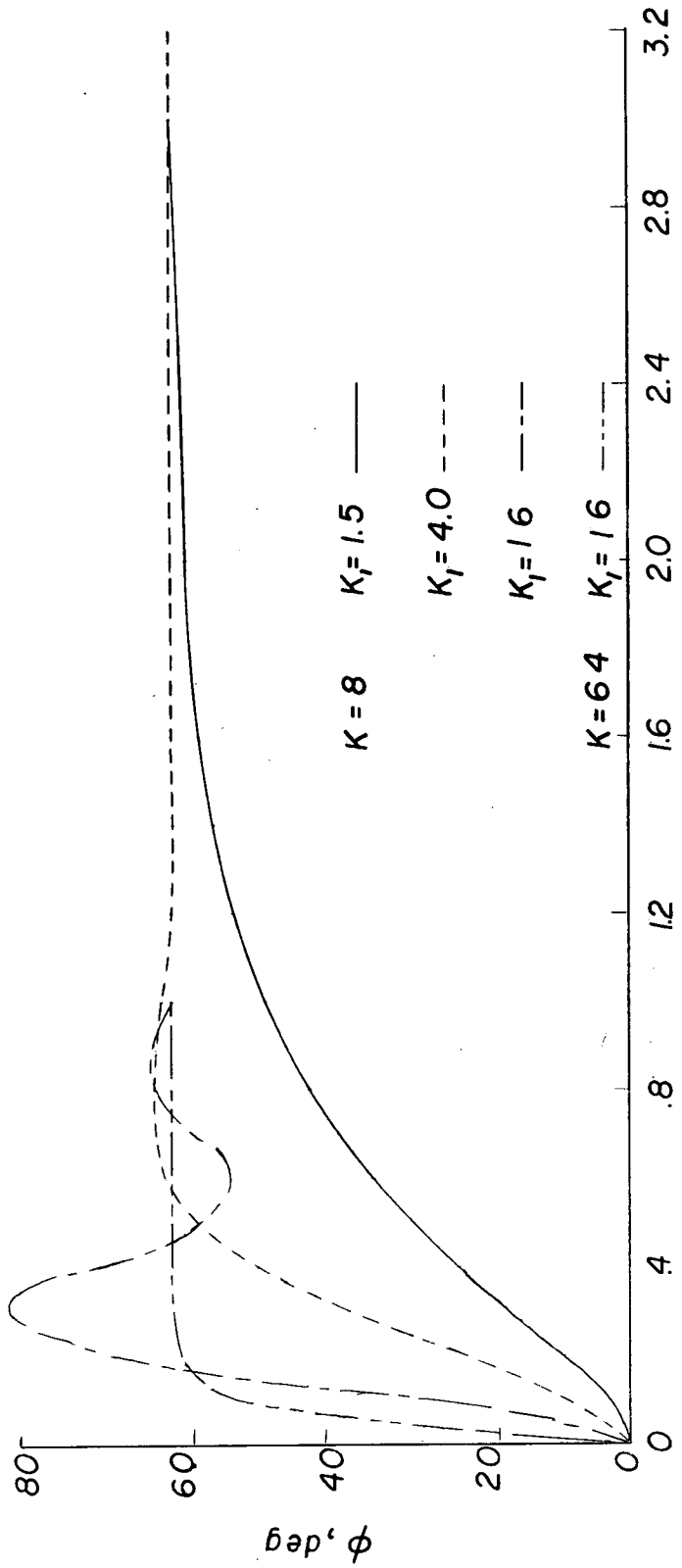

(b) Effect of varying K and K_1 for τ = 0.01 second.

Figure 13.- Concluded.

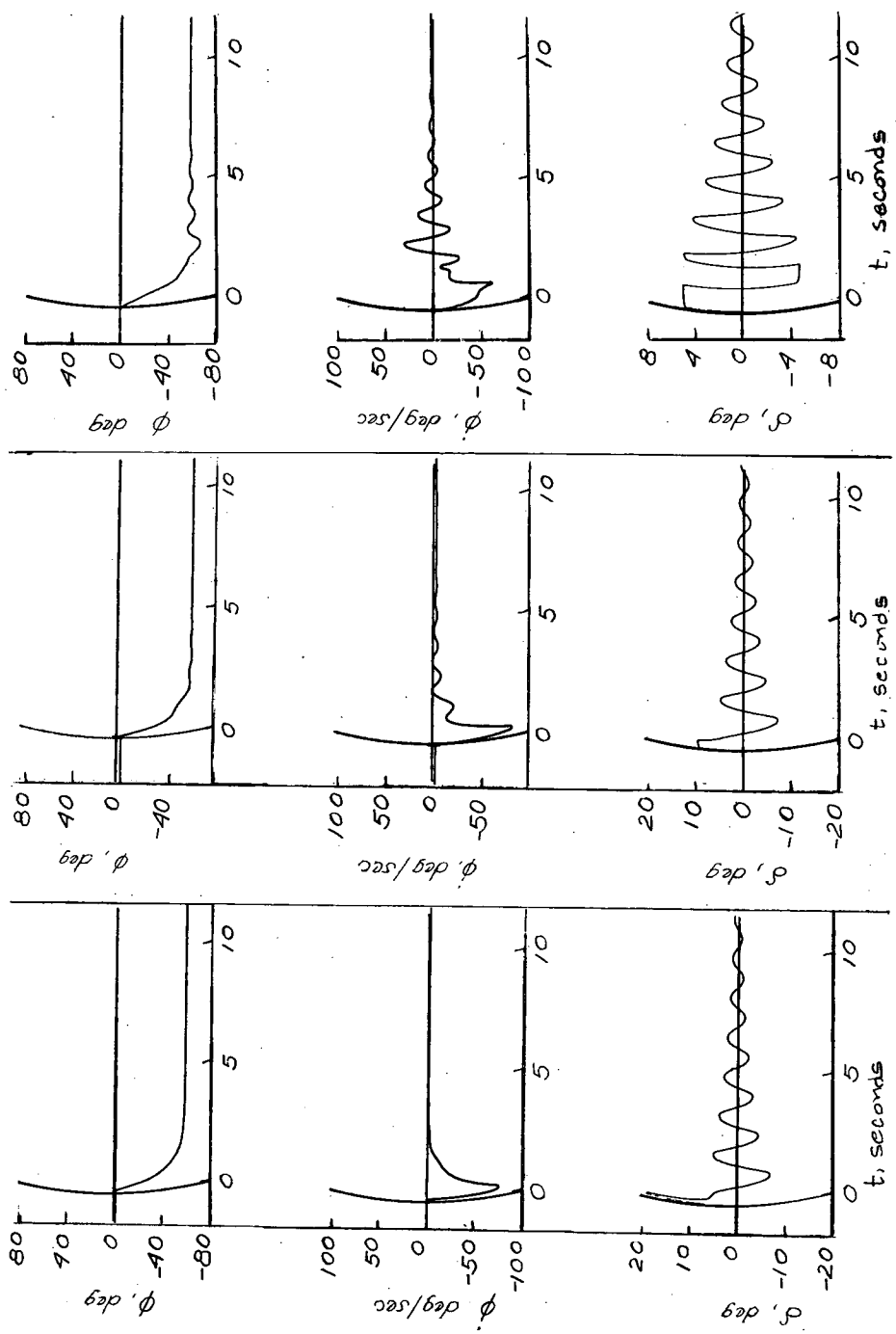

Figure 14.- Effect of limiting of δ on the response of the n = 2 velocity control system. K_1 = 1.5; K = 14; τ = 0; flight condition A; step input ϕ_i = 60°; $\dot{\delta}_l = \infty$.

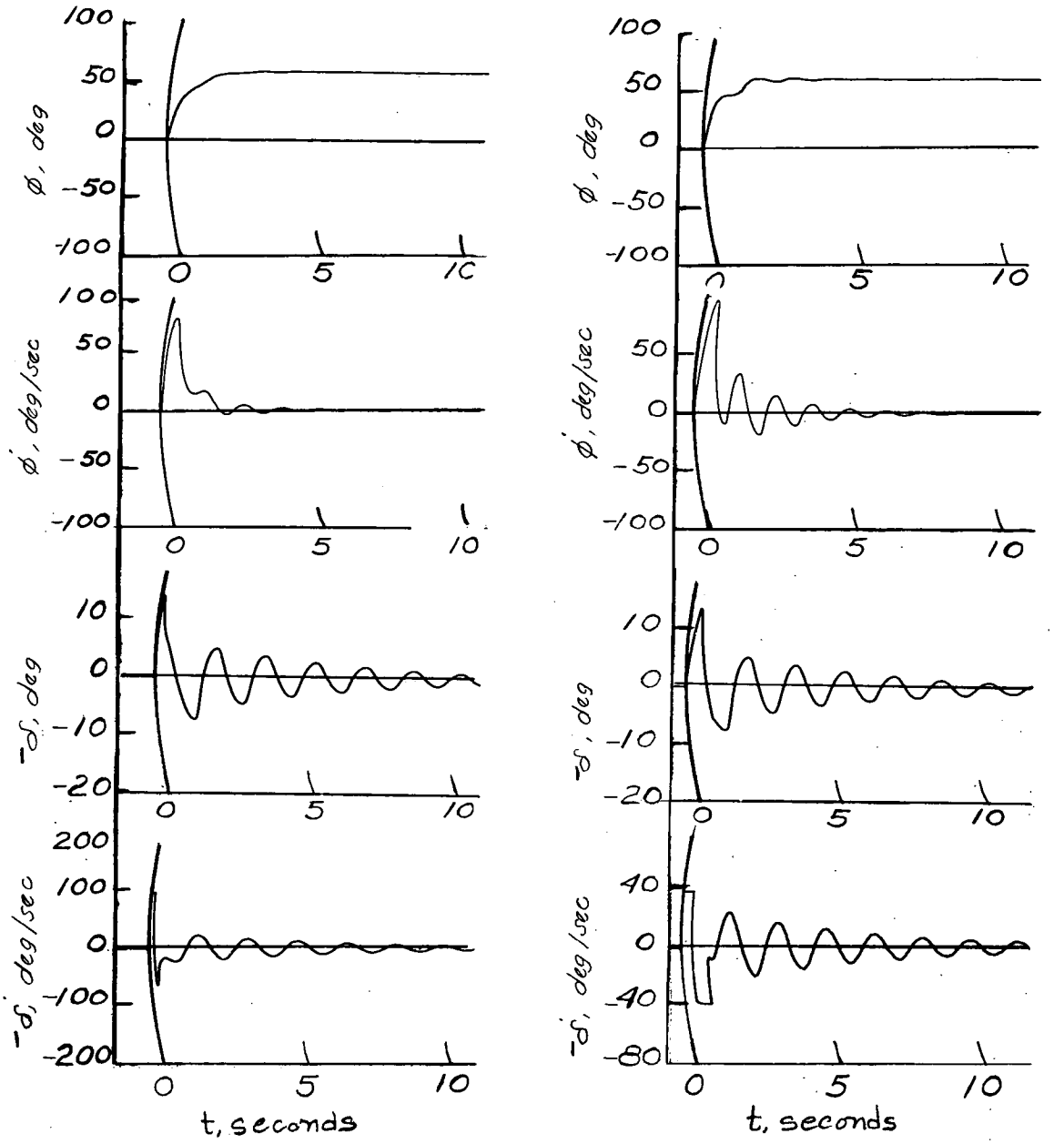

(a) $\delta_l = 20^\circ$; $\dot{\delta}_l = 100$ deg/sec. (b) $\delta_l = 20^\circ$; $\dot{\delta}_l = 40$ deg/sec.

Figure 15.- Effect of limiting of $\dot{\delta}$ on the response of the n = 2 velocity control system. $K_1 = 1.5$; $K = 8.0$; $\tau = 0.01$ second; flight condition A; step input $\phi_i = 60^\circ$; nonwinding limiter.

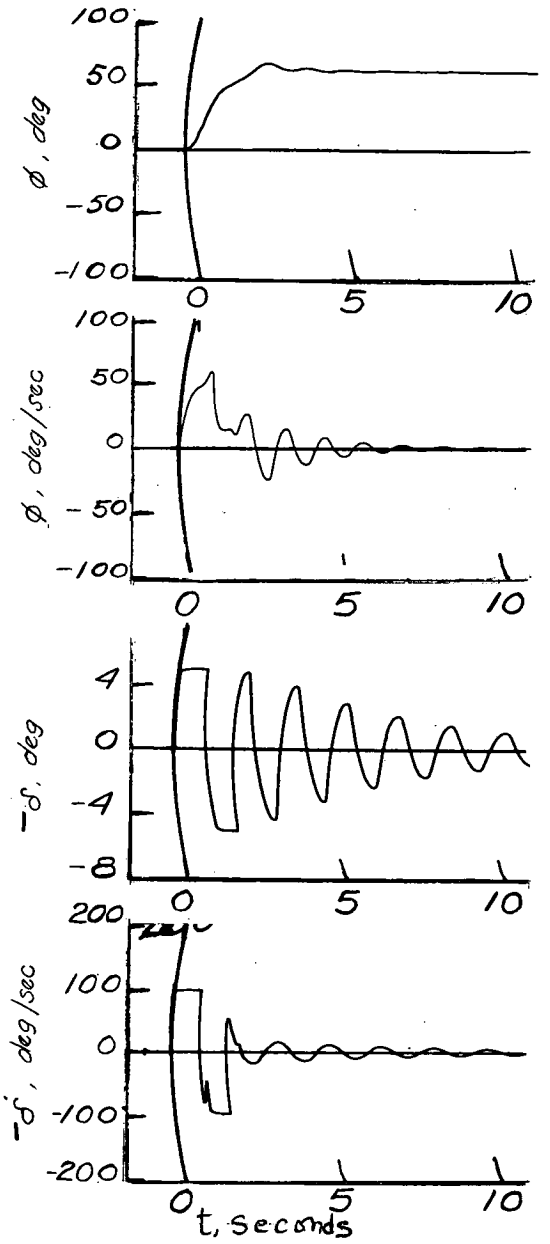

(c) $\delta_l = 5^\circ$; $\dot{\delta}_l = 100$ deg/sec.

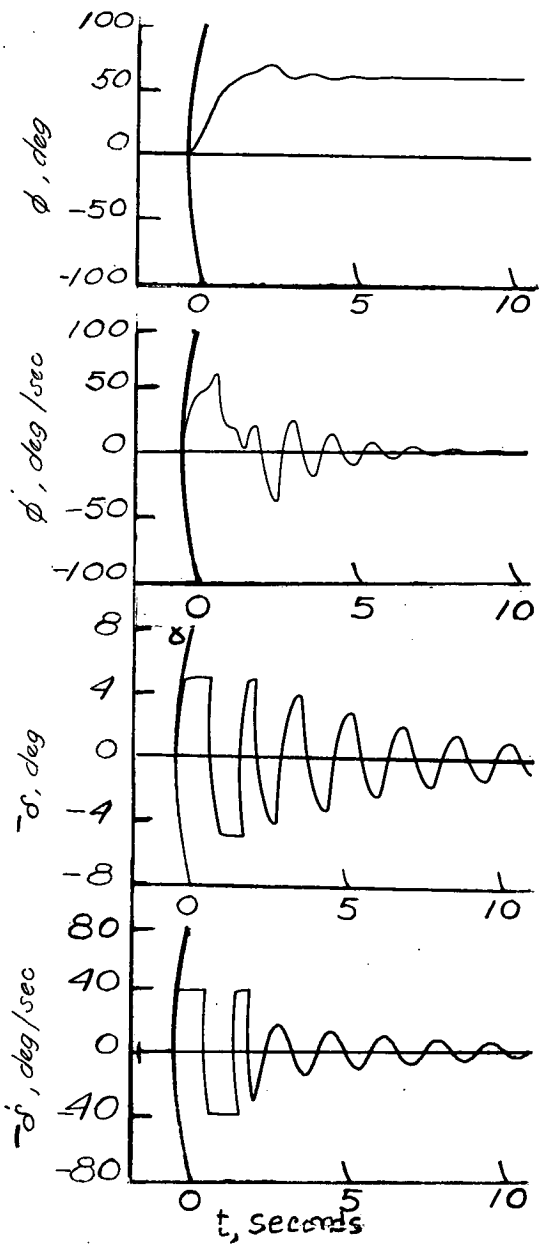

(d) $\delta_l = 5^\circ$; $\dot{\delta}_l = 40$ deg/sec.

Figure 15.- Concluded.

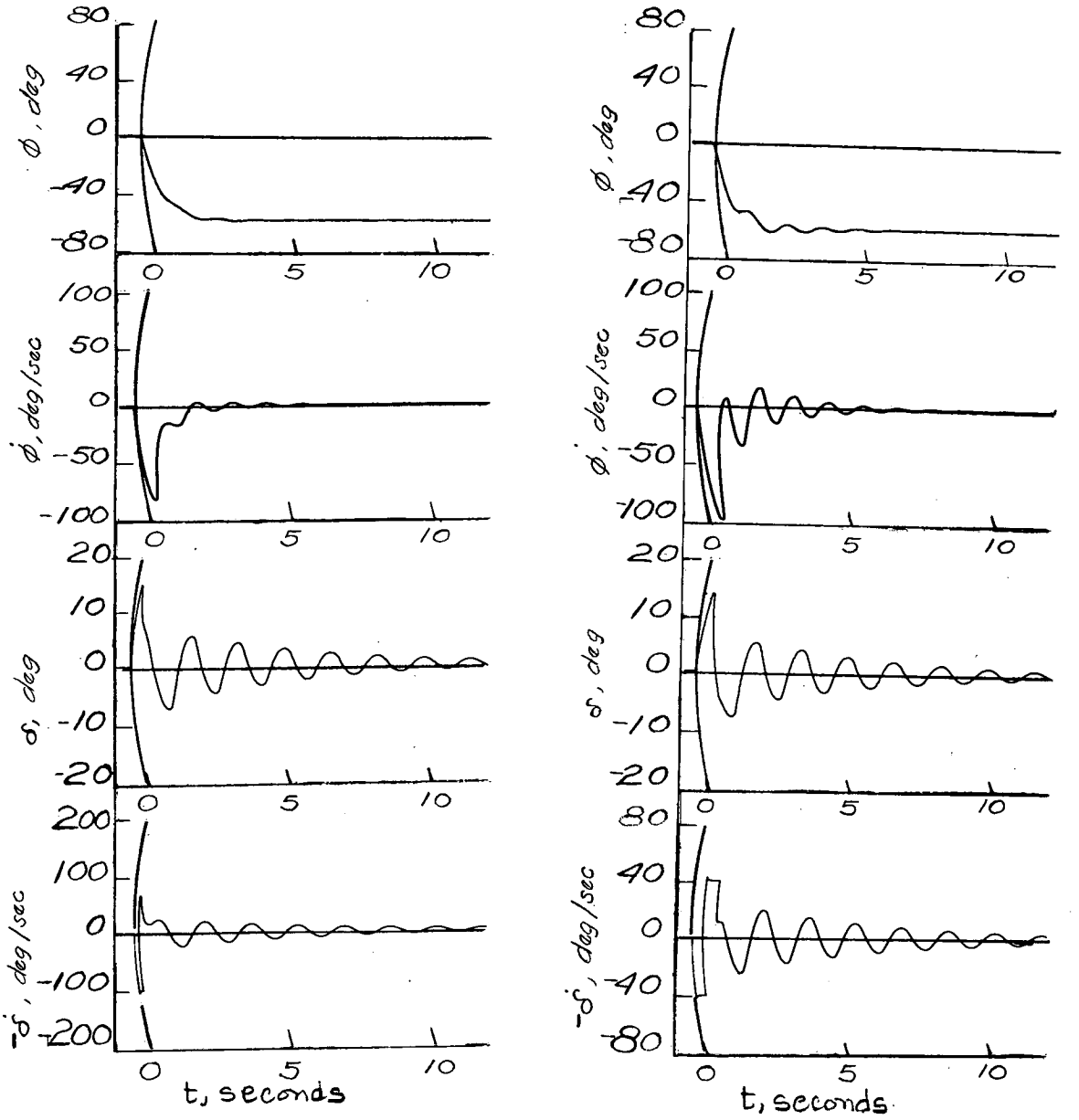

(a) $\delta_l = 20^\circ$; $\dot{\delta}_l = 100$ deg/sec. (b) $\delta_l = 20^\circ$; $\dot{\delta}_l = 40$ deg/sec.

Figure 16.- Effect of limiting of $\dot{\delta}$ on the response of the n = 2 velocity control system. $K_1 = 1.5$; $K = 8$; $\tau = 0.01$ second; flight condition A; step input $\phi_i = 60^\circ$; winding-type limiter.

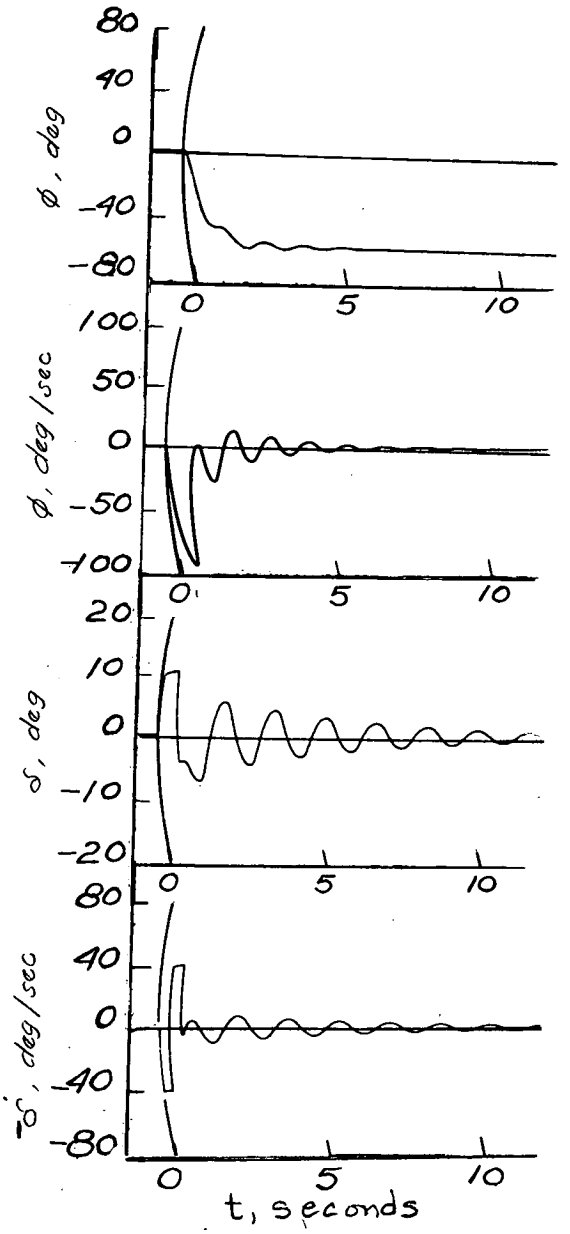

(c) $\delta_l = 10^\circ$; $\dot{\delta}_l = 100$ deg/sec.

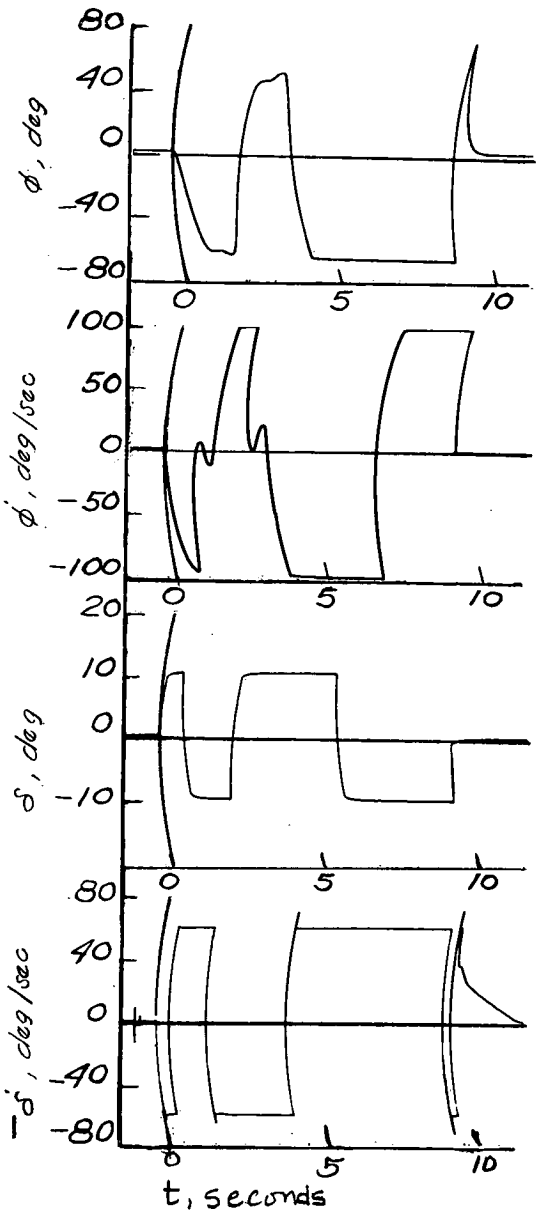

(d) $\delta_l = 10^\circ$; $\dot{\delta}_l = 60$ deg/sec.

Figure 16.- Concluded.

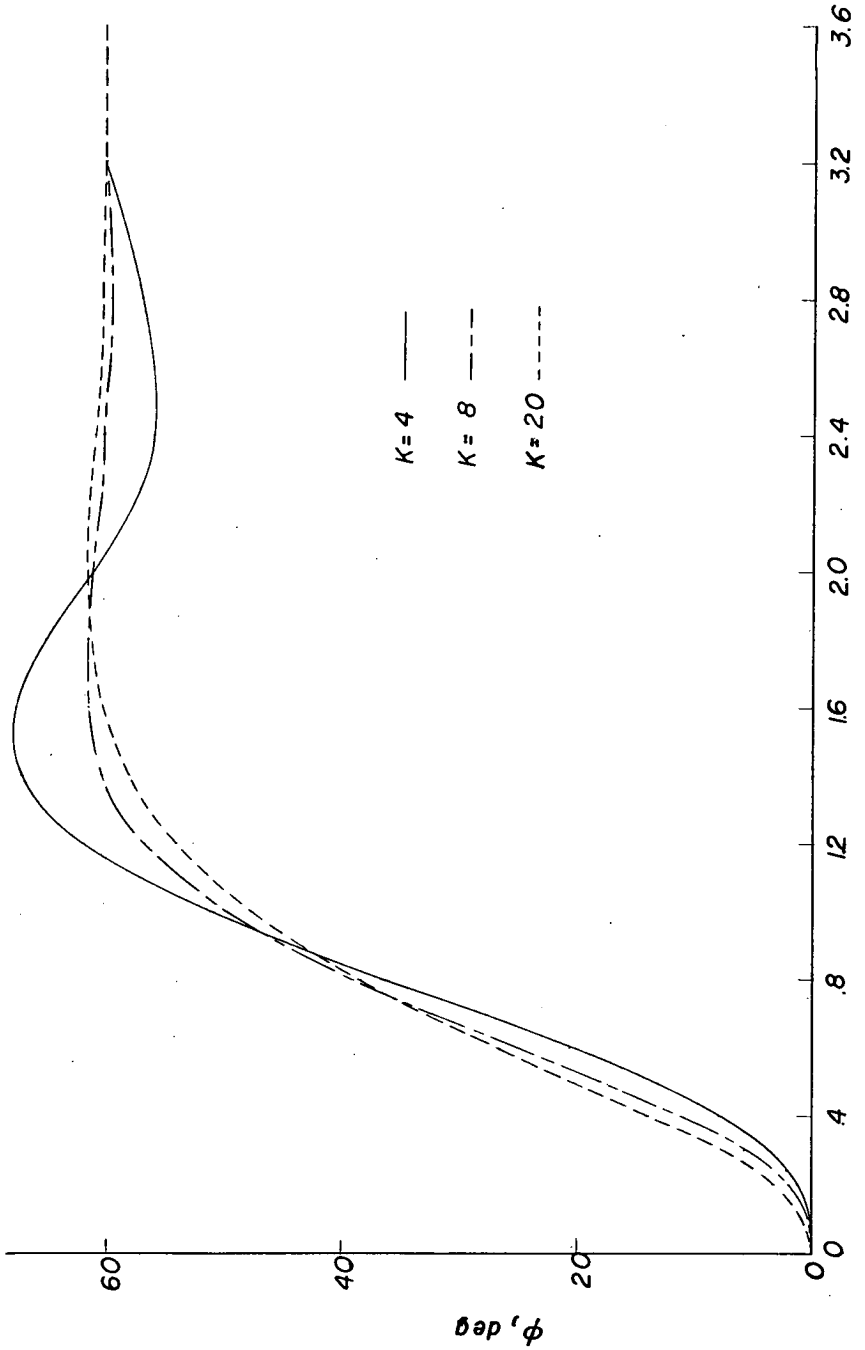

Figure 17.- ϕ response of the n = 3 acceleration control systems for various values of K. $K_1 = 1.5$; $K_2 = \frac{10}{3}$; $\tau = 0.01$ second; flight condition A.

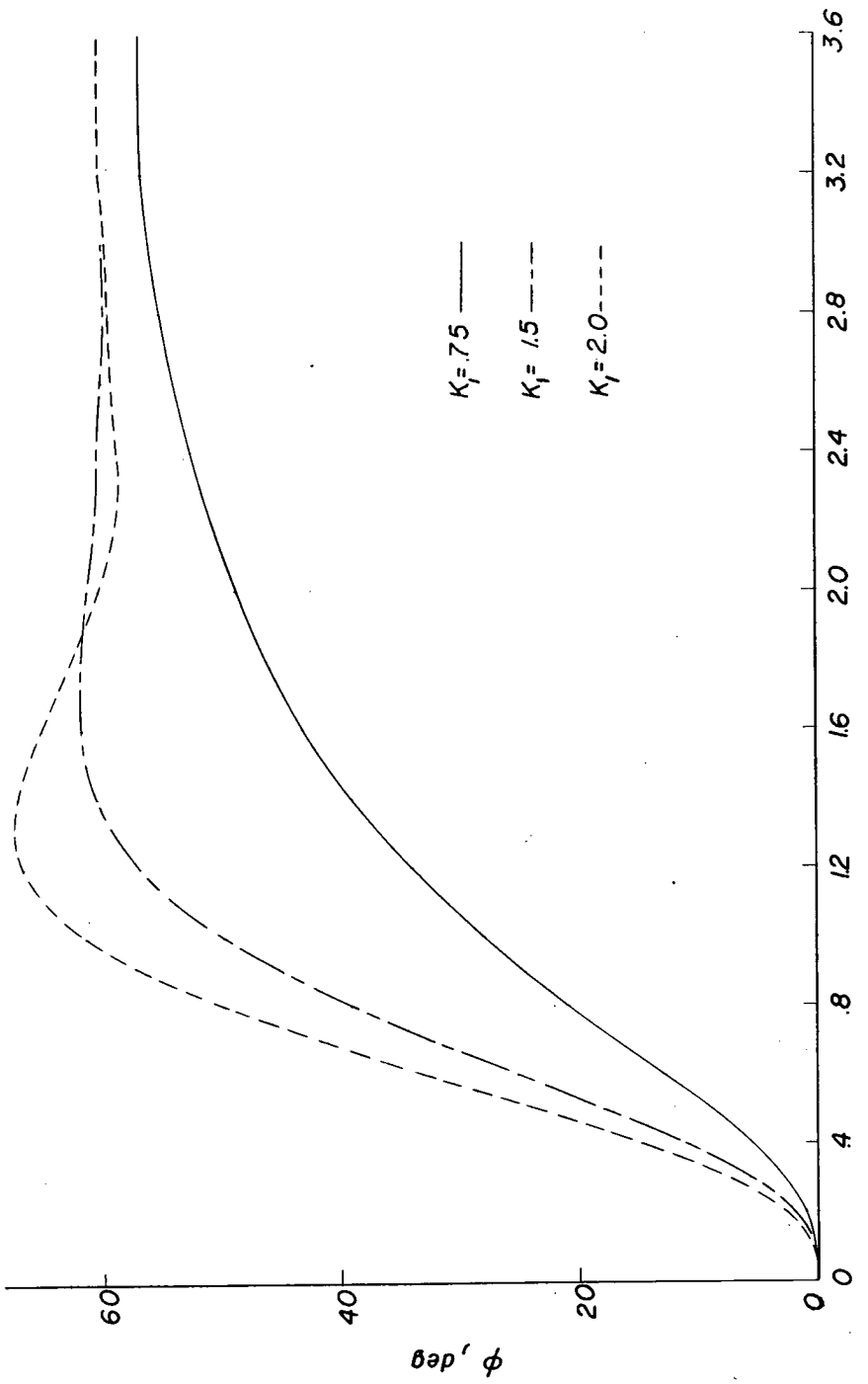

Figure 18.- ϕ response of the n = 3 acceleration control system for various values of K_1. $K_2 = \frac{10}{3}$; K = 8.0; τ = 0.01 second; flight condition A.

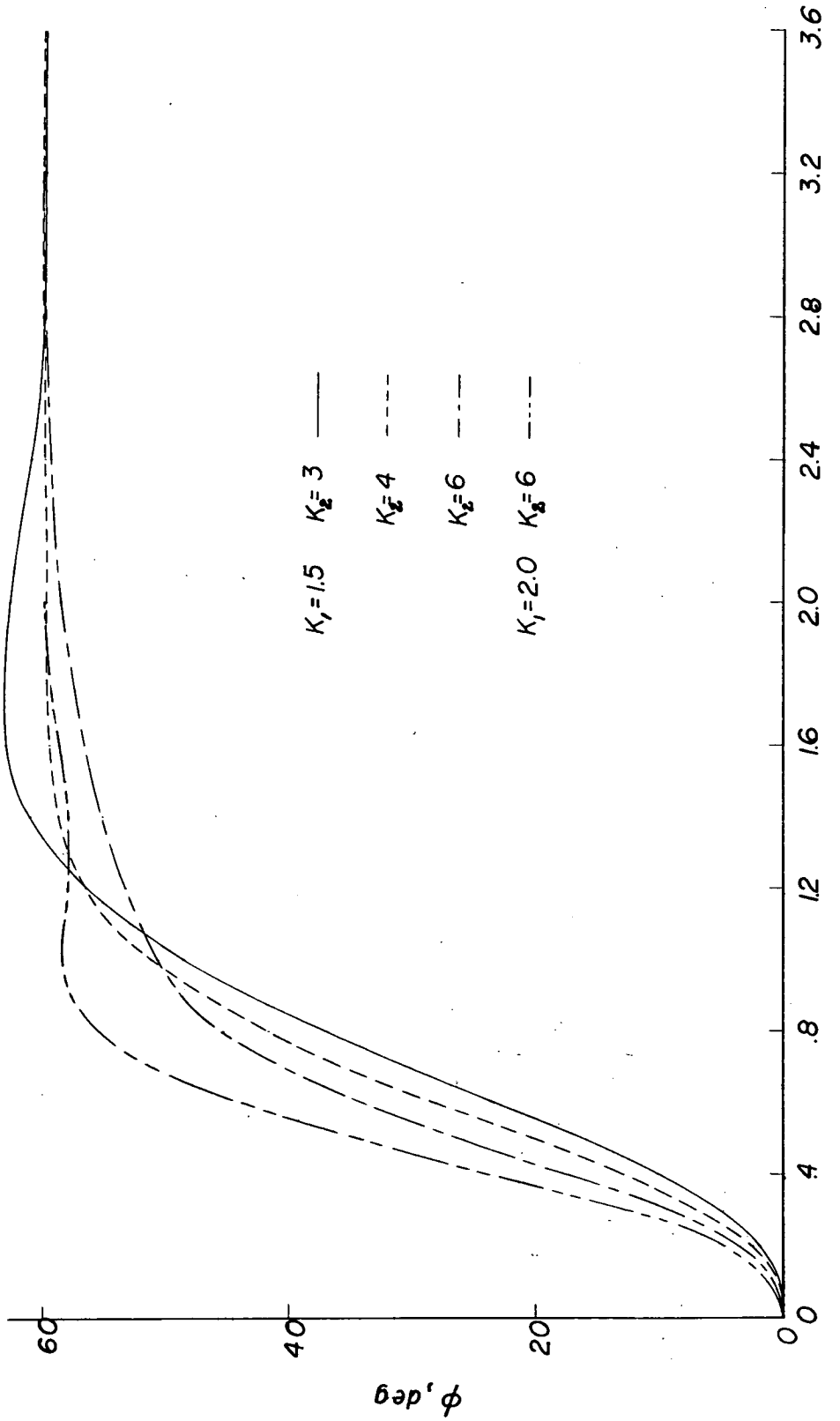

Figure 19.- ϕ response of the acceleration control system for various values of K_2 and K_1. K = 8.0; τ = 0.01 second; flight condition A.

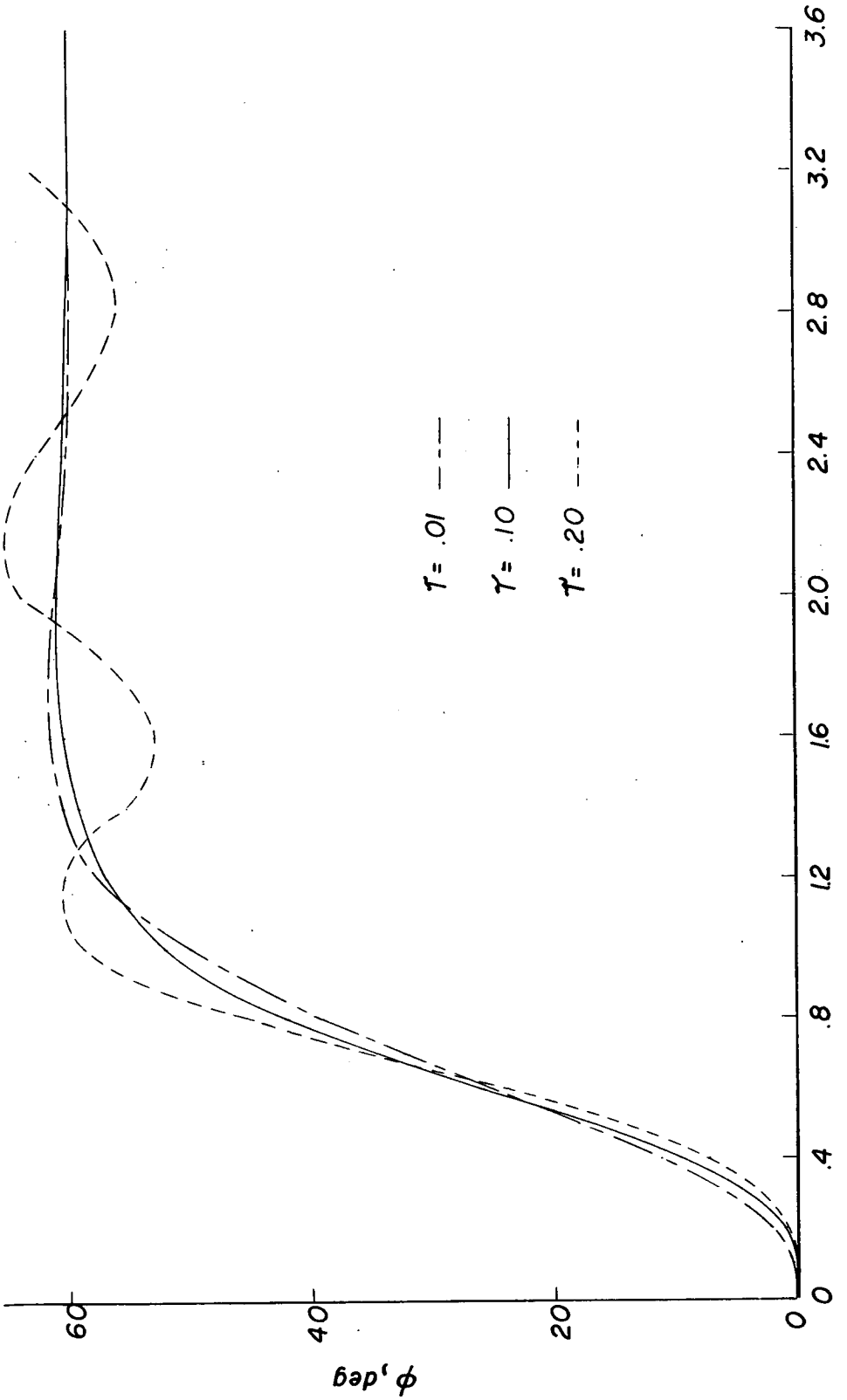

Figure 20.- ϕ response of the n = 3 acceleration control system for various values of τ. K = 1.5; $K_2 = \frac{10}{3}$; K = 8; flight condition A.

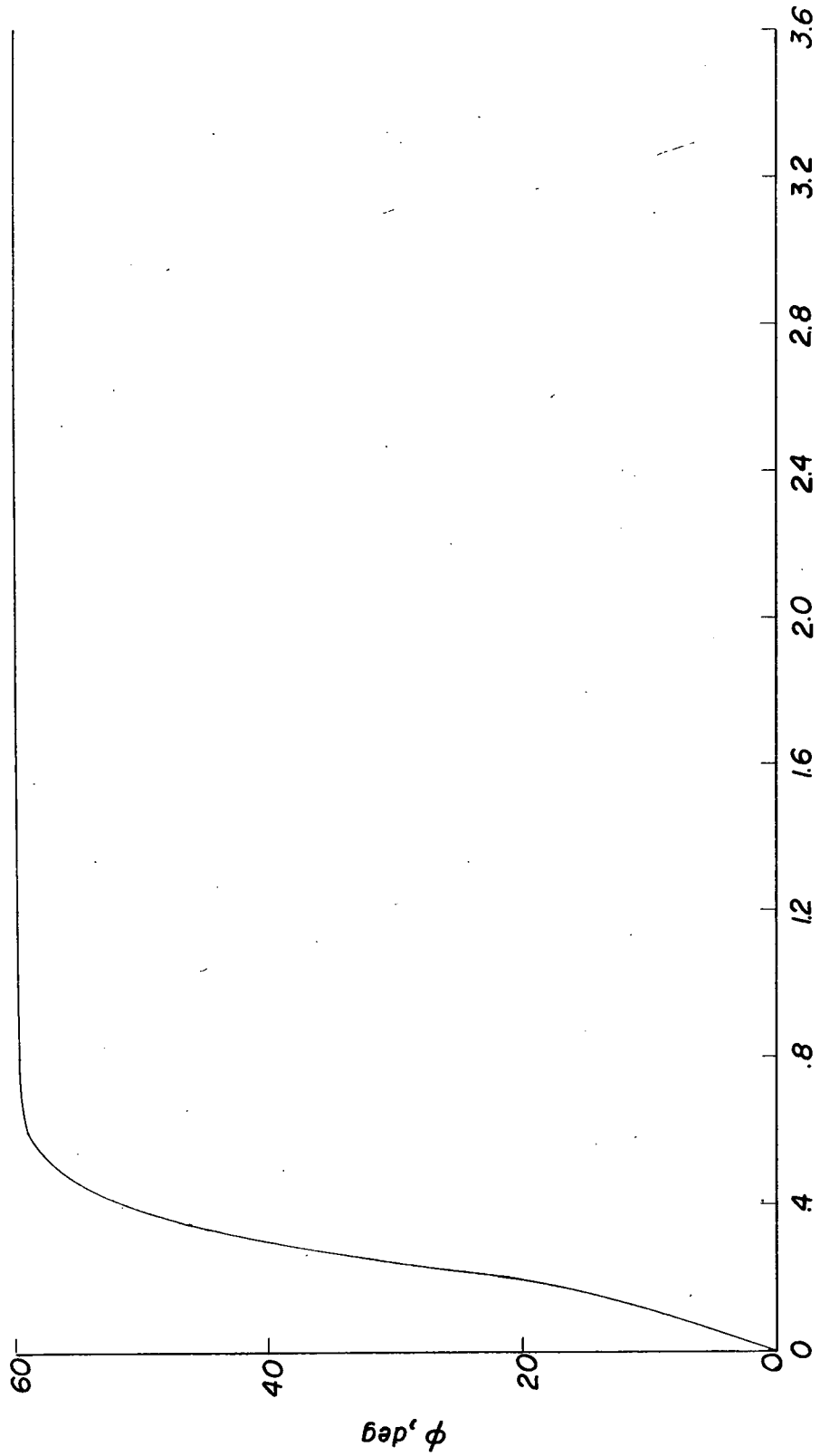

Figure 21.- ϕ response of the n = 3 acceleration control system. $K_1 = 3.75$; $K_2 = 10$; $\tau = 0.01$ second; flight condition A.

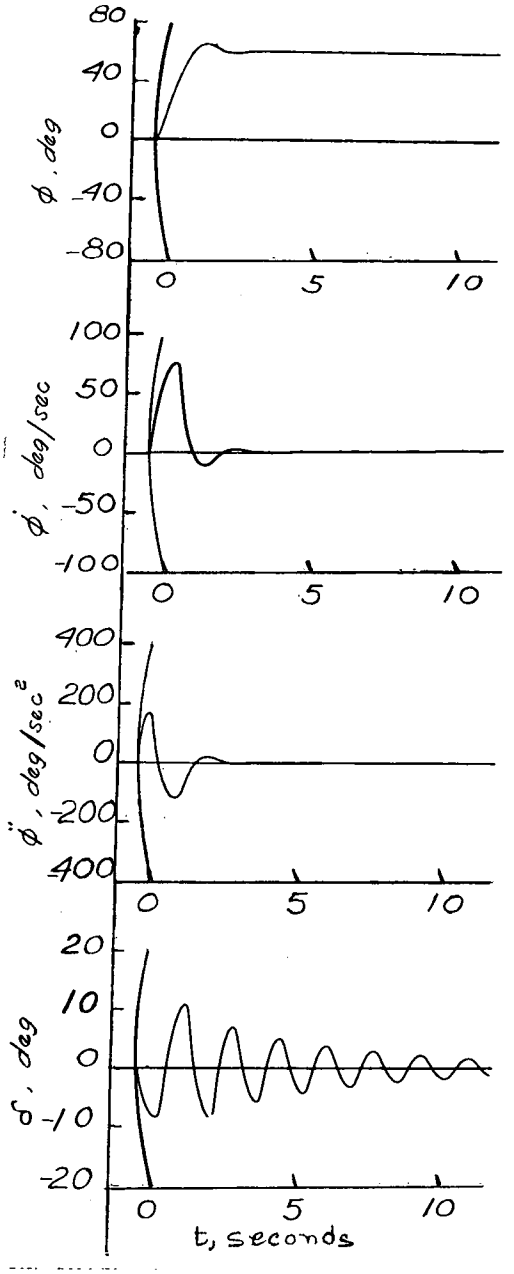

(a) $\delta_l = 20^\circ$.

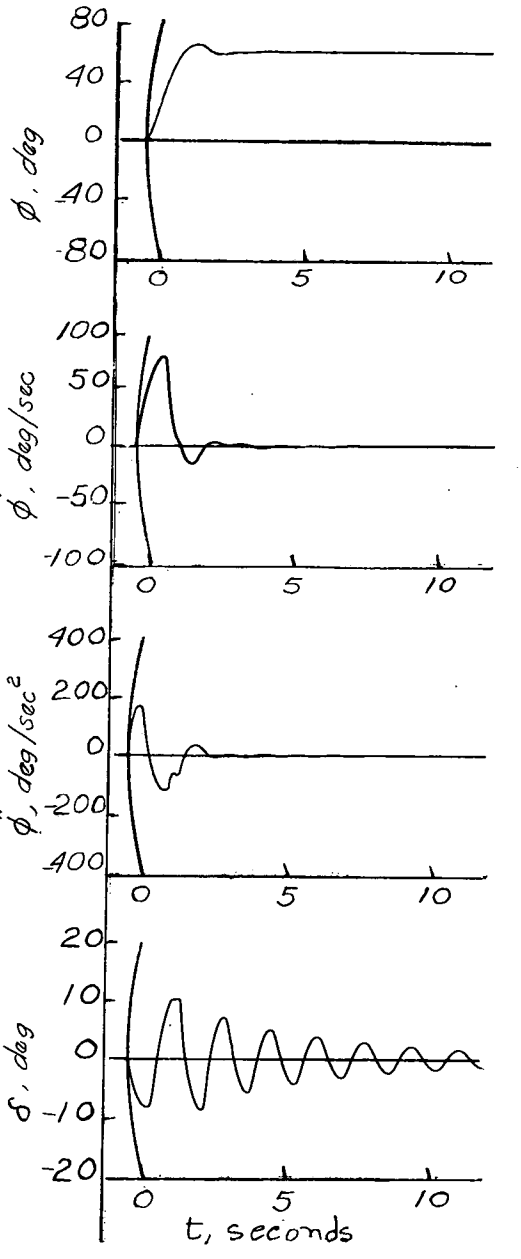

(b) $\delta_l = 10^\circ$.

Figure 22.- Effect of limiting of δ on the $n = 3$ acceleration control system. $K = 5$; $K_1 = 1.5$; $K_2 = \frac{10}{3}$; $\tau = 0$; flight condition A; step input $\phi_i = 60^\circ$; $\dot{\delta}_l = \infty$.

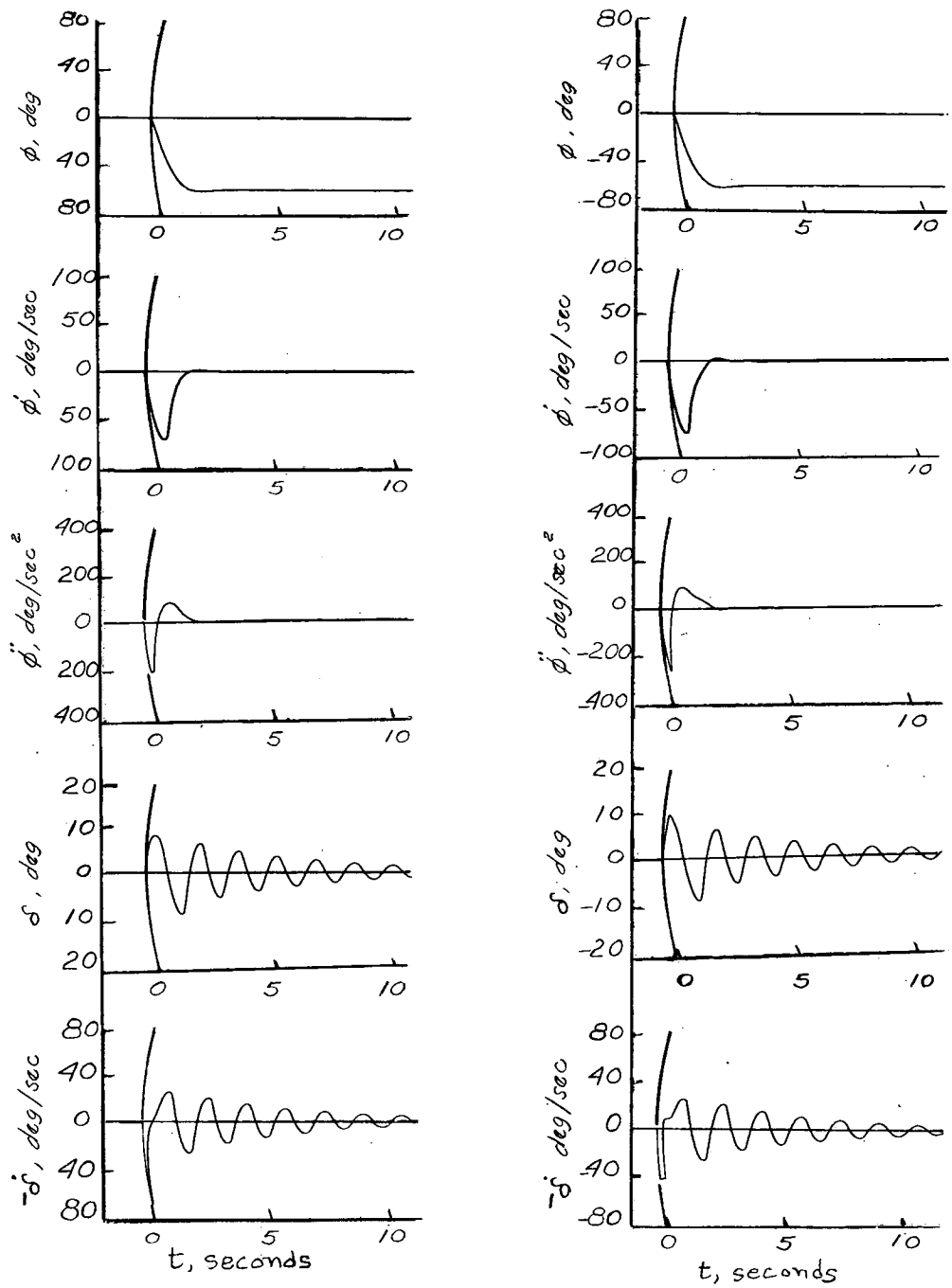

(a) $\dot{\delta}_l$ = 100 deg/sec. (b) $\dot{\delta}_l$ = 40 deg/sec.

Figure 23.- Effect of limiting of $\dot{\delta}$ on the response of the n = 3 acceleration control system K = 1.5; $K_2 = \frac{10}{3}$; K = 10; τ = 0.01 second; flight condition A; step input $\phi_i = 60^\circ$; $\delta_l = 20^\circ$; winding-type limiter.

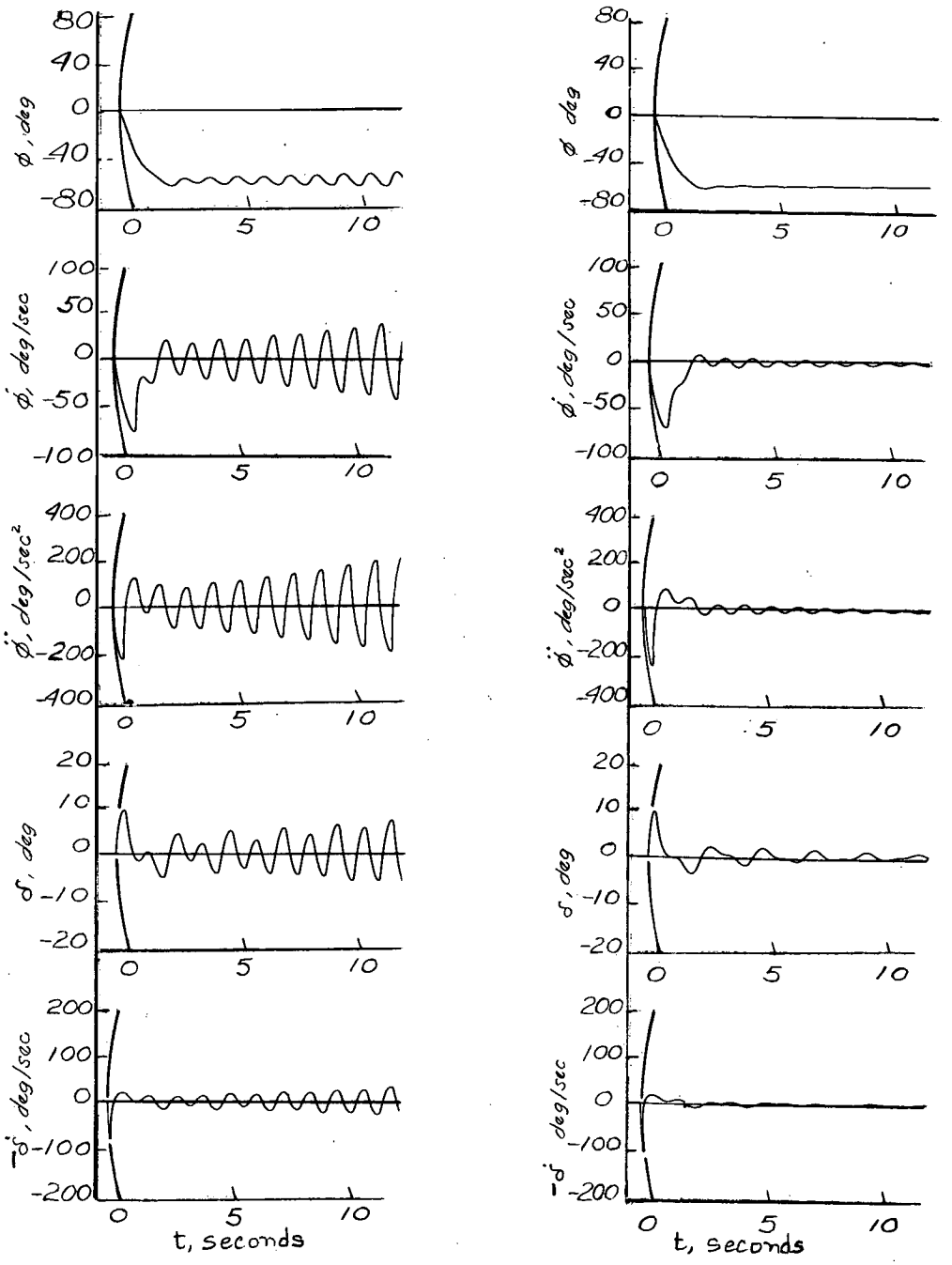

(a) K = 14. (b) K = 24.

Figure 24.- Effect of incomplete compensation on the response of the n = 3 acceleration control system. $K_1 = 1.5$; $K_2 = \frac{10}{3}$; $\tau = 0.1$ second; flight condition A in compensating network; flight condition B in airframe; step input $\phi_i = 60^\circ$; winding-type limiter; $\delta_l = 20^\circ$; $\dot{\delta}_l = 100$ deg/sec.

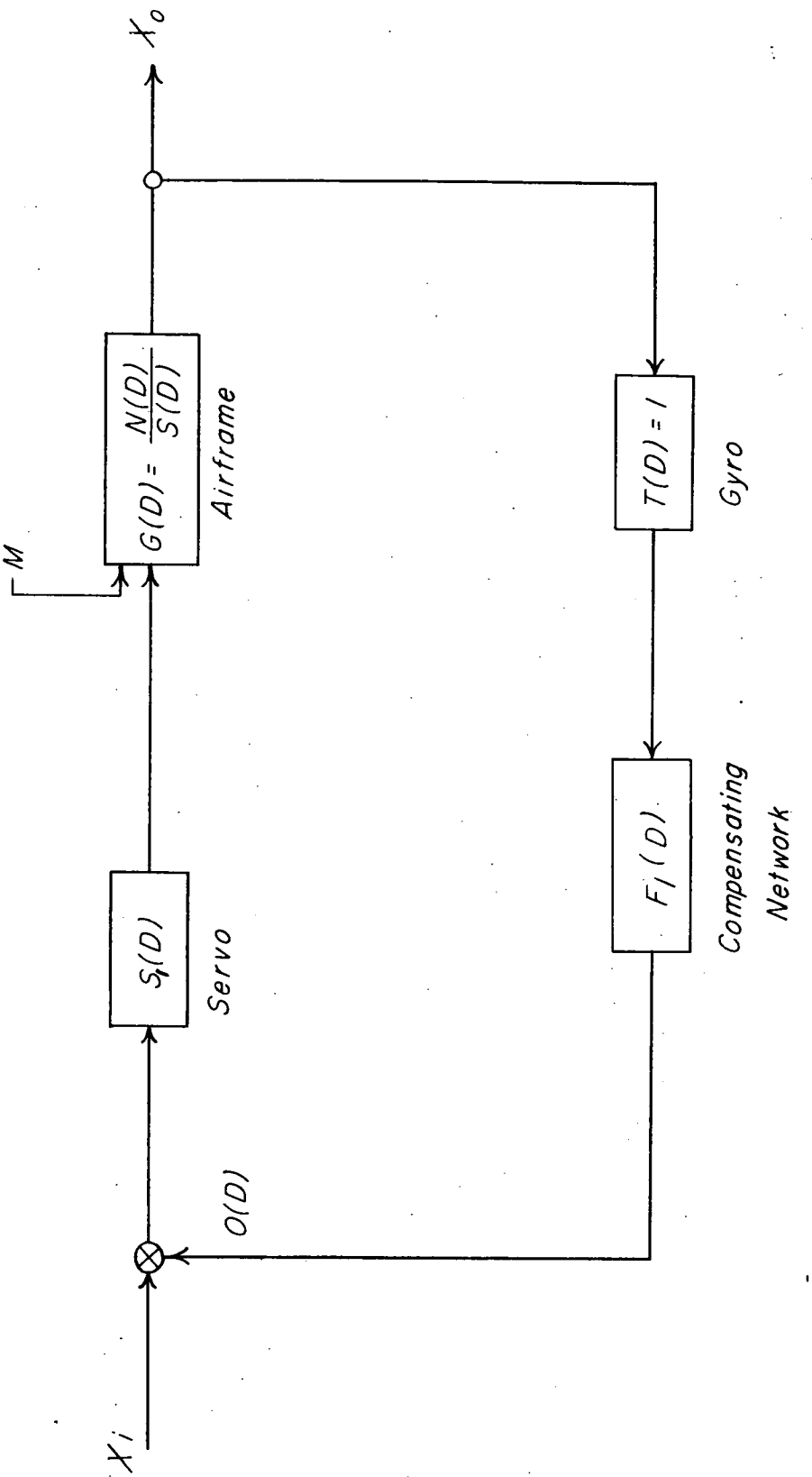

Figure 25.- Automatic control system incorporating a feedback-loop compensating network.

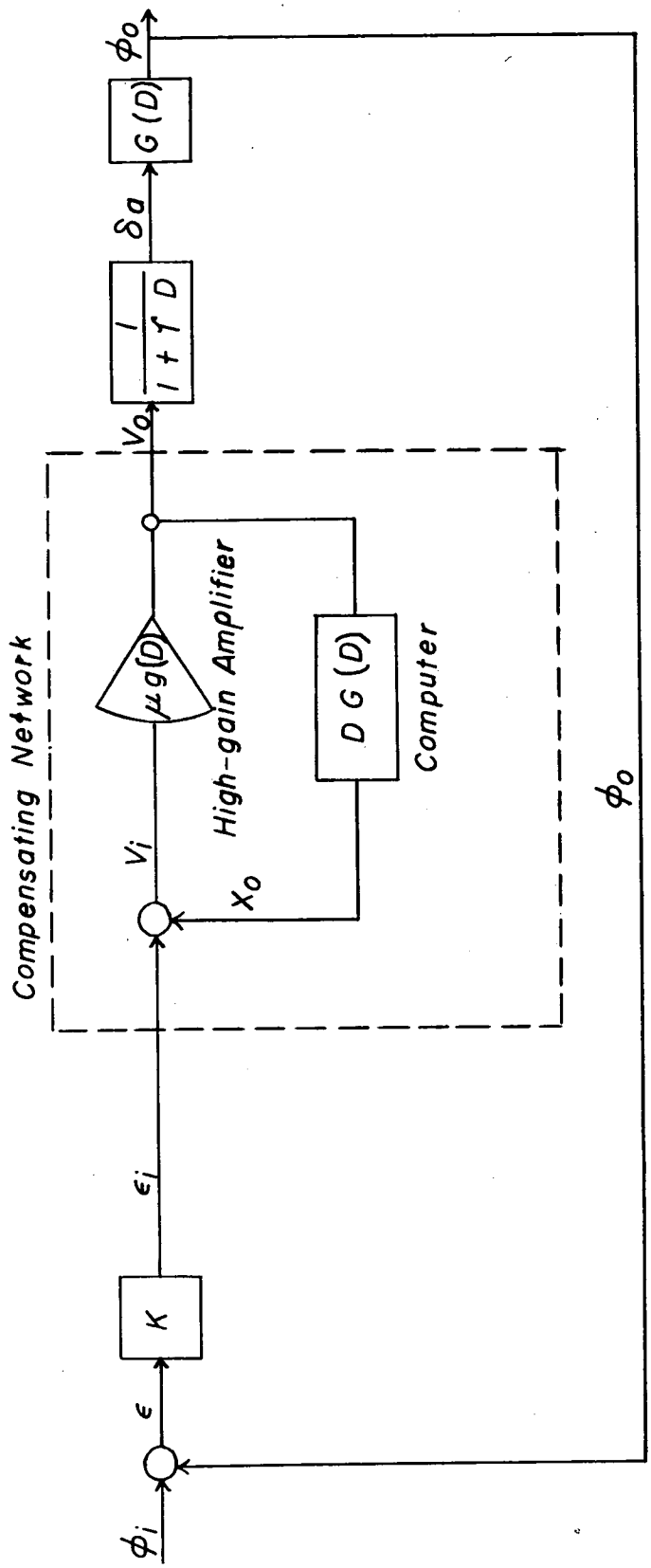

Figure 26.- Block diagram of displacement control system as set up on the REAC.